Hydraulics Affecting Bedrock Erosion at a Stream Knickpoint

Abstract

Bedrock erosion rates are generally considered to be proportional to local stream power. The actual erosion processes are influenced by sediment load, turbulent eddies, and other factors that influence how suspended sediment particles abrade the bed. Analysis of potential knickpoint erosion was conducted by a detailed study of both form and hydraulic processes along a series of knickpoints. To evaluate form, measurements of bed topography were surveyed along the longitudinal profile. Also a detailed bed topographic map was made by combining longitudinal surveys and cross section surveys of bed topography. These maps will include the location of potholes, exposed bedrock, and the distribution and size of bed particles. The evaluation of process comes through a survey of the water surface profile and cross sectional area for a major flood that Occurred on Oct 7-8, 2005. From the water surface gradient, cross sectional areas, and discharge obtained from survey and gauging station data, the following hydraulic characteristics will be calculated: flow depth, velocity, local shear stress (T/w), local stream power, flow resistance, and dimensionless shear stress. These hydraulic data were plotted as a function of longitudinal distance to evaluate the location of hydraulic features and bedrock morphology. Gradient, flow depth, and flow resistance in the longitudinal profile can be used to evaluate whether the flow is skimming flow or plunging flow and the consequences of flow type for bedrock abrasion.

Ashley Ann McCleaf

Advisor: Dr. Karen Prestegaard

April 14, 2006

Geology 394H

I. Introduction

A knickpoint is an abrupt steeping of gradient and it is often interrupted as a localized increase in erosion. Even on a longitudinal profile constructed by a 20-foot contour interval topographic map, these features are prominent (see figure 1). (Hence forth, we will be referring to the knickpoint closest to sea level as the Piedmont-Coastal Plain Boundary Knickpoint, the next the First Step Knickpoint, and the last the Second Step Knickpoint.) The First Step and Second Step Knickpoints are situated so that its base is bedrock. In order for these two knickpoints to migrate, bedrock must be eroded. Bedrock erosion is governed by the bed resistance to erosion, the slope of the channel, and the discharge through that channel. This makes the bedrock erosion a study of localized hydraulic conditions given that the Step Knickpoints are all of the same rock makeup. What exactly are those hydraulic controls on knickpoint migration, which influence bedrock erosion, is the main question being investigated in this paper.

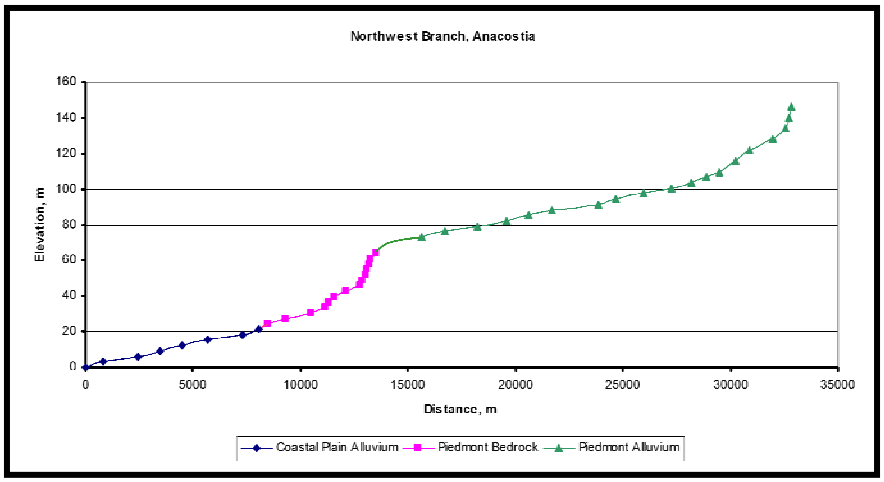

Figure 1. Longitudinal Profile of NW Branch of the Anacostia River (Prestegaard).

II. Previous Work

i. Knickpoint Initiation

Bedrock knickpoint origins tend to be where there is a difference in substrate competence, triggered by a change in base level. In this region, the Piedmont-Coastal Plain boundary is the most likely candidate for the origin for these knickpoints (Frankel 2001). This contact is known as the fall line (see figure 2). Where Coastal Plain sediments meet the metamorphic rocks of the Piedmont, a juxtaposition of substrate competence leads to a slight increase in gradient caused by differential erosion. From there, a downward component in erosion causes a faster increase in gradient and a knickpoint is formed.

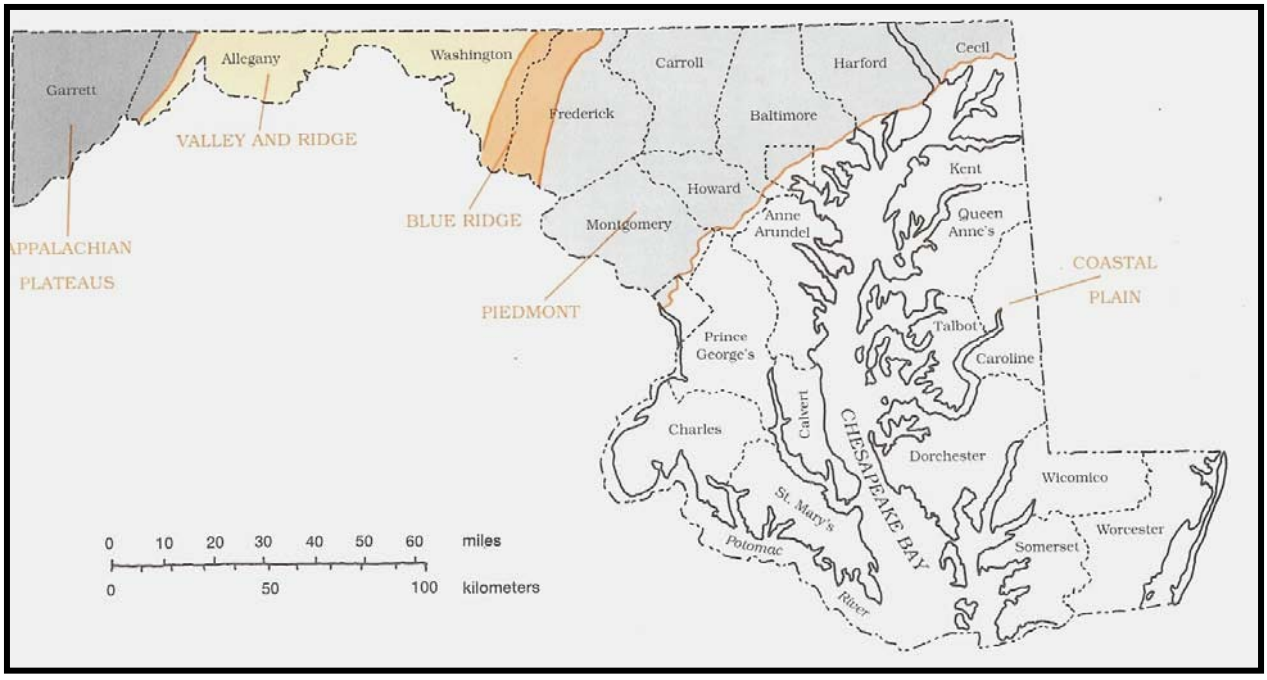

Figure 2. Fall line denoted as the boundary between the Piedmont and Coastal Plain Boundary (Maryland Geology).

Because the knickpoint is contained with the relatively homogeneous substrate of the Piedmont metamorphic rocks, variations in the weathering processes of abrasion and pothole coalescence become the dominate processes. The Northwest Branch of the Anacostia River cuts into the Loch Raven and Oella Schist (a biotite-plagioclase-muscovite-quartz schist) of the Glenarm Group, which also includes the Setters Schist and Cockeysville Marble (Schmidt 1993). Because of the relatively homogenous lithology, we are able to study the erosion and migration of bedrock knickpoints by localized hydraulic conditions.

Knickpoints tend to be studied as possible indicators of the tectonic history in a region (Phillips 2003, Schoenbohm et al 2001, van der Beek et al 2001). Flume studies of knickpoint retreat also have had a tectonic rationale (Frankel 2001, Pasternack 2004). Yet our study scale is on the order of meters and over a time interval of a few hundred years, thus making the tectonic explanation of migration too large and too long to be applied. Localized hydraulic conditions, which influence migration of bedrock knickpoints because of localize erosion, have not been studied to the point of publication. Therefore to understand the localized conditions created by a bedrock knickpoint, waterfalls must be researched.

ii. Localized erosion

Regionally, a stream's erosive ability tends to be evaluated by the power that stream can generated. The major variables in that equation are slope and discharge (see Methods). But regionally evaluating a stream only allows for an average picture of the stream's erosive ability. Bedrock streams have various ways in which it will erode on the scale on 1-2 meters and lower. Whipple (1998) writes that these processes are plucking, hydraulic wedging, bashing, abrasion,

cavitation, and solution. Plucking generally takes place where rocks are well jointed. Hydraulic wedging is another small scale process by which water moves into cracks and slightly expands due to heating and the rock breaks apart. Sediment bashing usually happens on a small scale, yet can happen to large boulders under high flows. Erosion by abrasion has the suspended load slamming against the bed. Cavitation is not something that can be intuitively understood. It is when vapor bubbles find a point of low pressure and then collapse. When this happens a suctioning affect ensues and this suction can pull off pieces of the bedrock. Solution erosion is typical chemical weathering when there is a dissolving of the bedrock from something which is dissolved in the river. In addition to these methods of erosion of bedrock streams is a relatively new idea: pothole coalescence (Springer 2004). This erosion type is when many potholes form in a localized area and over time they align. During high flow, it strips the rock between two pothole "lines". The two types of erosion that we will be studying in detail are abrasion and pothole coalescence.

Johnson (2004) writes "abrasion by sediment in turbulent flow often sculpts bedrock channels into dramatic forms." Abrasion needs a clear bedrock surface, so some process must sweep the sediment off an area for a long period of time for abrasion to become affective. Hancock, Anderson, and Whipple (1998) believe that abrasion is proportional to velocity to the fifth power

$$A \propto V^5$$

where A = abrasion and V = velocity. In order for abrasion to be a dominate process in stream erosion, its velocities must be high. This leads to the assumption that the majority of abrasive erosion occurs during high flow when the stream's velocity is at its peak, given from the increase in discharge during high flow.

Pothole coalescences also needs a clear surface in which to function. In order for a pothole to deepen and widen quickly, sediment needs to get trapped inside of it, acting as a tool. This bashing affect causes the pothole to become more uniform, regardless of variation in the bed its cutting through. There is a paper by Springer which comes to the conclusion that pothole coalescences is the major process by which the South African Orange River knickpoint erodes over time (Springer 2004).

iii. Bedrock channel morphology studies

At the knickpoint's location, the channel is incised. The width is constricted by the bedrock surrounding the channel on three sides. This channel also contains larger boulders which could have come into place from earth flows or from the plucking of larger boulders from the bedrock by the channel during high flow. The understanding of large sediment's relation to incision controls and channel morphology controls are necessary backgrounds needed to understand the localized conditions at the knickpoints.

The large sediment within the stream and channel width constriction are related and can be mathematically evaluated by the used of the "top sum" variable (Clancy 2004). This variable relates the largest particles, over D84 (the 84^{th} percentile size of sediment diameter), to their ability to "jam" and cause a blockage in the stream. A particle jam makes the large sediment less mobile and it also protects the underlying bedrock from erosion. Larger boulders in the stream cause an increase in channel gradient and a narrowing of a valley over time (Madeji 2003). This narrowing of the valley is the incision of the bedrock stream into its base where the particle jam does not exist, usually down stream of the particle jam. Typically if a substrate's resistance is

high, the channel will grow narrower and deeper. Large particles also tend to influence bed and wall topography and cause more localized erosion in the form of potholes, longitudinal grooves, and a steeper, more variable bed gradient (Wohl et al 2002). It has also been noted by Wohl (1998) that reaches where the bed is more resistant have more knickpoints and stepped morphology.

Bedrock channel morphology is governed by the same hydraulics as other stream types, yet its response to those hydraulics are typically different. The reduction of stream power is not through large meanders as we would see in Coastal-Plain streams, rather through step-pool/ riffle-pool sequences (Chin 1998, Zimmerman et al 2001). As a result, we find variability in sediment distribution and gradient (Canavan 1989).

iv. Plunging versus skimming flow

All of these variables apply if and only if the flow during the flood is uniform. Yet after the flood, there was one inconsistency between a theoretical model of the area and the actual flood. The step or plunging flow did not occur over the bedrock knickpoint, but over the particle jam which is situated above the knickpoint. This inconsistency led to more research which uncovered a FEMA presentation (Reichmuth 2005) which is still in the process of being published (see figure 3). The authors found that a particle jam can force two different types of flows.

a. **Plunging flow:** This flow concentrates the stream power at the base of the particle jam and organizes the turbulent flow into a pothole/potholes downstream. Plunging flow is usually associated with waterfalls.

b. **Skimming:** The second scenario is skimming flow. This allows the stream power and shear stress to be uniform over the area and abrasion would have to be considered uniformed. It results in a large pothole to form close to the particle jam.

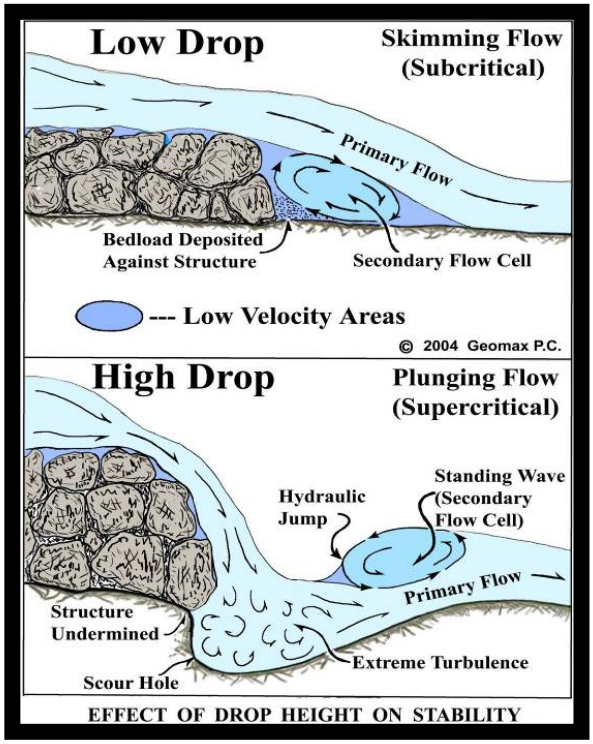

Figure 3 Flow Type from FEMA paper yet to be published (Reichmuth 2005)

v. Waterfall recession as an analog to knickpoint migration

A waterfall is a large scale knickpoint. Its recession has been a well studied phenomenon. Yuichohi Hawayakawa (2003) wrote on waterfall recession rates at the Boso Peninsula in Japan

shows that there can be a ratio derived from the erosive force of stream to the bedrock resistance. The erosive forces in a waterfall can be studied through variables such as discharge, the width and height of the waterfall, and the unconfined compressive strength of the bedrock. Niagara Falls is another location where waterfall recession is well studied. Most models and hypotheses are lithology driven (Boyd 1928, Cazeau et al 1965, Spencer 1908 & 1898).

The problems associated with using a classical waterfall approach is that knickpoint migration is not lithologically dependent and that the knickpoint only acts as a waterfall at very high flows. Waterfalls by definition are an area with a very steep gradient where the water separates from the bedrock. This means that the free fall of the water does not erode away the area of increasing gradient; rather it undercuts itself to propagate itself headward. This is where a plunge pool would form. Fleeger (2001) investigated on the origins of Archbald Potholes in Lackawanna County, Pennsylvania, and discussed multiple hypotheses of the two larger potholes as a result the carving of a plunge pool at the base of an inclined Moulin and the carving by subglacial melt water. Most knickpoints are not waterfalls. They do not have a separation of flow from the bed. This flow separation influences how erosion acts on the bed, therefore studying waterfall recession as an analogue to knickpoint migration cannot be a primary support for this study.

III. Hypotheses

Bedrock erosion is influenced by sediment load, turbulent eddies, and other factors that influence how suspended sediment particles abrade the bed. The hypotheses for how this occurs at a channel knickpoint are:

1. Knickpoints erode primarily through simple abrasion concentrated at narrow parts of the stream. Therefore, abrasion is proportional to local stream power and suspended sediment load.
2. Bedrock erosion is localized at pothole locations and knickpoint migration occurs as result of pothole coalescence. Therefore, the flow hydraulics must generation significant macro-turbulent eddies that stationary in terms of their position on the bedrock channel.
3. Bedrock knickpoint location is influenced by the jamming of large bed particles above the knickpoint. This jamming of particles locally protects bedrock from erosion, but it can also affect longitudinal profiles

- Research has been conducted with the assumption that the middle knickpoint is the site with the most active erosion and headward migration, because the middle knickpoint is kept clear of sediment, exposing its bedrock at all times; contains a larger population of potholes, flutes, and scour marks; and has a large pool at its base.

IV. Methods

i. Study Site

Figure 4. Satelite view of Burnt Mills.

The Burnt Mills section of the Northwest Branch of the Anacostia River is located approximately one mile west of the New Hampshire Avenue-Route 29 intersection in Montgomery County, Maryland (See figure 3). It is

approximately 10 minutes from the University of Maryland College Park campus. This stream was chosen because it contains two prominent bedrock knick points and it crosses the Piedmont-Coastal Plain boundary. The section is between two tributary junctions and incised to bedrock so there is no groundwater flux; therefore, the discharge is constant through the reach. The reach is also within 10 minutes of campus and is on public land. The reach also has two USGS gauging stations; one above and one below it. This makes flood work easier because there are approximately 60 years of data to analyze. From October 7^{th}-8^{th}, 2005 there was a 5 year recurrence interval flood. Given the gauging station data, a discharge value can be calculated for the reach. The greatest advantage of using this reach is that it is manageable. Field work at low flow, such as surveying, and high flow, such as taking pictures and flagging, can be conducted safely.

ii. Channel and bed morphology

In order to test the simple abrasion hypothesis, a variety of techniques are used. First a great deal of field data must be accumulated in order to construct a detailed, 2-dimensional longitudinal profile of the area (similar to figure 1). Second, an actual flood must be measured and surveyed for high flow hydraulic calculations. The use of the Hyattsville gauging station allows us to construct a flood frequency graph normalized to drainage basin area. From that graph we can calculate actual discharge in the region. Finally a stream power and stream stress calculations must be done to identify what sized sediment can be moved during high flow.

a. Cross sections

While out in the field, detailed surveys on all scales must take place. A cross-section is the most elemental of the stream characteristics that is noted. Cross-sections are taken approximately every 10 meters, with additional cross-sections taken at closer interval when the stream becomes more complex. The line level technique is used with one foot increments taken in width to measure the depth of the bed and the low water surface.

Error on the cross section occurs through natural variability and operator error. We cannot truly account for natural variability, especially given the terrain that the cross section was taken over (see figure 5). Given that the depth was taken with a standard, a stadia rod, the measurement error would be ± 1 cm. In order to assess operator error on width measurements were taken 6 times each for two different widths. On the 15 meter cross section, the variability was ± 2 cm (0.13% error). The 30 meter cross section would naturally contain more error because of the slack that may accumulate in the tape measure. Its error was ± 3.5 centimeter (0.12% error). Thus, the measurement error is considerable smaller than the natural variability. It is the natural variability in width and depth that is the goal of the measurement program.

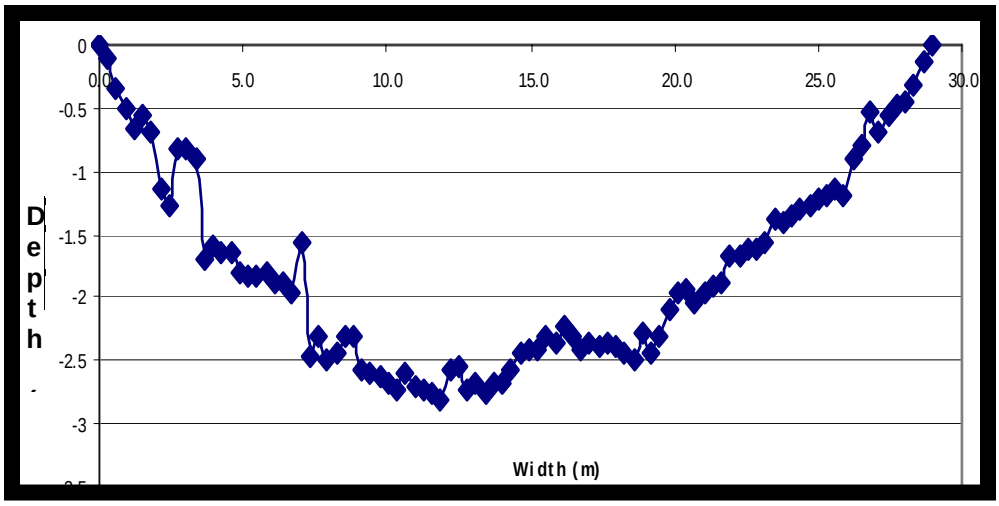

Figure 5 Cross Section at 64 meters. Error within data points.

b. Bed and water surface surveying

A broader survey that must be done is the bed and water surface longitudinal survey Using a survey transit, both water surface and the bed profile were taken at ~2.5 meter intervals. Benchmarks are taken approximately every ~30 meters. Each cross-section location is also surveyed.

The flood elevations of the October 7-8, 2005 flood were also surveyed along with the bed and water surface elevations. Flood elevations were photographed during the peak of the flood. After the flood, these photographs were compared with field evidence of high water marks, such as sand lines and floating debris lines (Styrofoam was particularly helpful). High flow markers were flagged and marked with the longitudinal distance, and their elevations were obtained by surveying techniques. This water surface profile was used to determine energy gradient during the flood: measurement error and correct identification of the surface. Two sources of error are associated with the survey elevations. Measurement error is the accuracy of reading the stadia rod elevation. This error ranges from 0.2 to 0.5 cm depending upon the

distance from the level. The other error derives from an accurate identification of the surveyed surface. For flood strand lines, this can vary by 1-2 cm. For the water surface elevation, this varies by less than 1 cm. The rough bed provides the greatest measurement error with slight variations in the choice of placement of the stadia rod give different bed elevations.

c. Particle size and organization

Grain size measurements were also made in the field. These measurements were made within the line of a cross section to establish both the grain size probability distribution and the position of particles within the cross section. To obtain grain size data, every particle was measured for its a- and b-axis along a cross-section line. Orientation of each particle is noted, which is whether the "A" axis was parallel or perpendicular to flow direction. Using a tape measure, the particles were measured in place, unless covered by another particle or sand. The error associated with a tape measure, after repeated trails was ± 0.3 cm.

d. Hydraulic measurements and calculations

From all of the field data accumulated, hydraulic calculations can be made. The first is average velocity. From the discharge calculated from the flood frequencies and the cross sectional area, it can be found that

$$V = \frac{Q}{A_f}$$

where V = velocity, Q = discharge, and A_f = functional area. Then using the calculated velocity and a slope and depth gained from the survey, flow resistance a dimensionless flow resistance coefficient will be gained from

$$\frac{\mu}{\mu^*} = \frac{\mu}{\sqrt{gRS}}$$

where μ / μ* = dimensionless flow resistance, μ = velocity, g = acceleration due to gravity, R = depth, and S = gradient.

Energy calculations can also be made. Stream power, which is directly related to abrasion, can be calculated from the discharge and slope

$$\Omega = \rho g Q S$$

where Ω = stream power, ρ = density of water, g = acceleration due to gravity, R = depth, Q = discharge, and S = slope/gradient. The area with the highest calculated stream power will be the one with the most active abrasion during floods.

For all of these calculations, the error comes from the measurements used as values in the equations.

e. Bed mobility

Calculations can be done to find the D84 of the entire system and find what the maximum sized particle that can typically be moved. Also, calculations of shear stress allow an analytical method to see if a certain particle could move. Shear stress is defined as

$$\tau = \rho g R S$$

where τ = shear stress, ρ = density of water, g = acceleration due to gravity, R = depth, and S = slope/gradient. Dimensionless shear stress, which is

$$\tau^* = \frac{\tau}{(\rho_s - \rho_w)gD}$$

where τ^* = dimensionless shear stress, τ = shear stress, ρ_s = density of sediment, ρ_w = density of water, g = acceleration due to gravity, and D = sediment size, has a set of accepted values for the movement of various particle sizes. For instance, gravel is given a value of 0.045. Again the error is associated with the measurements of the variables in the equation.

f. Bedrock morphology

Figure 6 Arial view of first step knickpoint.

Bedrock morphology is an observational study. Here the use of paleohydraulic indicators is most prominent. These features are abandoned and active potholes at both low and high flow, boulder arcs, flutes, scour marks, and terraces (See figure 6). By taking many photographs and surveying in the location of the various indicators, a short term hydraulic history may be inferred. The features will be plotted on the longitudinal profile to see if there are any correlations between the placement of these indicators and the high flow steps and/or high shear stress and stream power. If the shear stress and stream power are high enough to remove particles to expose the flat bedrock in the channel, vortices of similar magnitude activate and form potholes. Also given the two different types of flow the reach may have experienced during the flood, the location of the active potholes may provide additional evidence for a given flow type.

V. Results

In order to discuss the results of this project, it is necessary to divide the results into three sections. The first looks how discharge was calculated for the reach, including sources of error and comparisons to localized discharge. The second section focuses on the various cross sections and grain size distributions throughout the reach and what those two factors tell us about the hydraulics of the area. Finally, the third section discusses how depth, width, effective width, shear stress, stream power, and stream power per unit width vary as a function of longitude.

i. Determination of flood discharge and velocities from October 7th-8th flood

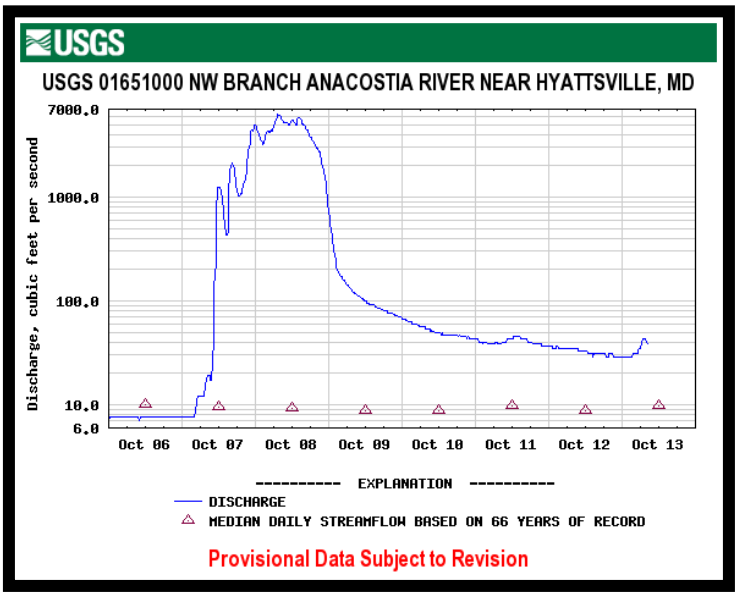

Figure 7 Hyattsville Gauging Station Hydrograph in 2005

Because discharge is constant throughout the reach, one discharge value can be calculated. Only one USGS gauging station was operational during the October 7-8th flood and that was the NW Branch Anacostia River near Hyattsville (station 01651000). The peak discharge was ~6,000 cubic feet per second (cfs) with a wide peak that lasted for ~12 hours (see figure 7). It is possible to take that discharge and apply it to a flood frequency curve created to find the recurrence interval of that flood (see figures 8 and 9). Next, a flood frequency curve is created which is normalized to

drainage basin area. We can take the recurrence interval of that flood and apply it to the graph to get a normalized value which can then be multiplied by the drainage basin area of the reach. To obtain a value for the drainage basin area, topographic maps of the region were used and drainage basin areas penciled in for the surrounding streams using the highest elevation as the dividing line. Then the area of the drainage basin was calculated by counting the number of 2 mm by 2 mm squares were in the outline and multiplying that value by the scale. This lead to 5,570 ± 100 cfs (157.8 ± 30.5 cubic meters per second) being the value for discharge for the flood.

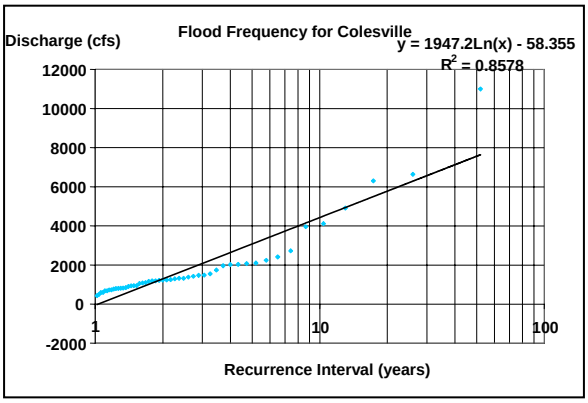

Figure 8 Flood Frequency Curve for Colesville Station

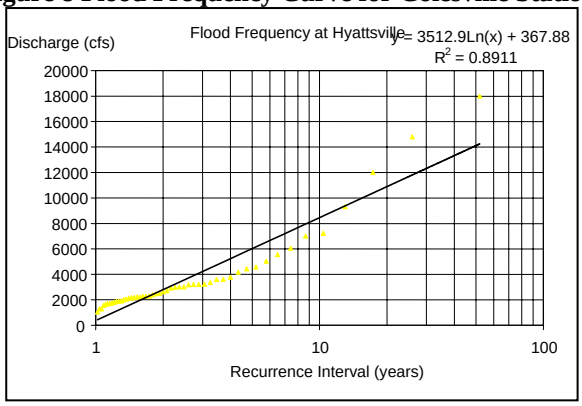

Figure 9 Flood Frequency for Hyattsville Station

The error for this value comes from the gauging station itself and from the extrapolation from the flood frequency curve and measured drainage basin area. The error in this perspective

seems very large; however, for this project the error on this value is not a major source of error in the analysis because the goal is to examine variations in shear stress and stream power through a reach in which the discharge is constant. The actual value of the discharge is constant throughout the reach and can be constrained by both the gauging station and watershed area method and local measures of cross sectional area and velocity during the peak of the flood. These values were quite similar, the estimate from the field cross section data is 5,500 ± 250 cfs (155.9 ± 76 cubic meters per second). This falls within the same range of values as the gauging station and watershed area method that was presented above.

ii. Flood cross sectional surveys and calculation of flood velocity and Froude Number

In total there were five detailed cross sections made, 19 flood and effective width combinations taken, and two grain size distributions formed. Since the discharge is constant through the reach and taken to be 158 m3/s , the variations from section to section in velocity are caused by differences in cross sectional area. The average velocity for the upper section was 5.65 ± 0.01 m/s and the lower section was 1.99 ± 0.15 m/s. (This reported error is due to the error in measurement of cross sectional area). At the end of the bedrock knickpoint, the average velocity was 7.89± 0.15 m/s. From the velocities, Froude Numbers can be calculated. There were two areas of supercritical flow (with a Froude number over 1), which were situated at the bedrock knickpoint and coming out of the Second Step Knickpoint (see figure 10). The supercritical flow tends to be over an area where bedrock is the only surface exposed to the water. In essence, the flow comes out of the largest knickpoint supercritical, moves to subcritical throughout the particle jam, becomes supercritical over the bedrock knickpoint, and finishes as

subcritical at the plunge pool. The inconsistent high flow survey demonstrated in the longitudinal profile below the knickpoint is a hydraulic jump, where the flow makes the transition to subcritical flow.

Distance (m)	Upper/ Middle Lower	Width (m)	Depth (m)	Area (m^2)	Discharge (cubic m/s)	Velocity (m/s)	Froude Number
17.50	U	18.28	1.30	23.76	157.80	6.64	2.25
64.00	U	22.56	1.50	33.84	157.80	4.66	1.11
70.00	M	10.00	2.00	20.00	157.80	7.89	3.17
75.00	L	19.51	3.70	72.19	157.80	2.19	0.24
82.80	L	29.00	2.50	72.50	157.80	2.18	0.24
85.88	L	33.65	2.90	97.59	157.80	1.62	0.13

Figure 10 Width and Froude Number Data

iii. Bed profile and water surface profile at high and low flow

The bed, low water surface, and high water surface profiles show an interesting picture (see figure 11). The particle jam and the bedrock knickpoint clearly stand out in the low water surface profile. The high water surface profile displays two important features. The first is skimming flow over most of the area except over the particle jam. Over the particle jam, the profile displays a plunging flow. This plunging flow forces the flow to become supercritical over the bedrock knickpoint into the plunge pool. Because of this, the second important feature of the survey can be explained, the bulge in the high water surface profile in the lower reach. This area is where the supercritical flow's compression is released as the flow becomes subcritical. This hydraulic jump was at first thought of as a mistake in surveying, but repeated surveys in the field resulted in similar values. Calculation of the Froude numbers explains this variation in flood elevations. These two features in the bed and water surface profiles point to an important

hydraulic feature, the particle jam, which should now be referred to as the boulder knickpoint. The stability of this zone must be evaluated now that this feature has become so important.

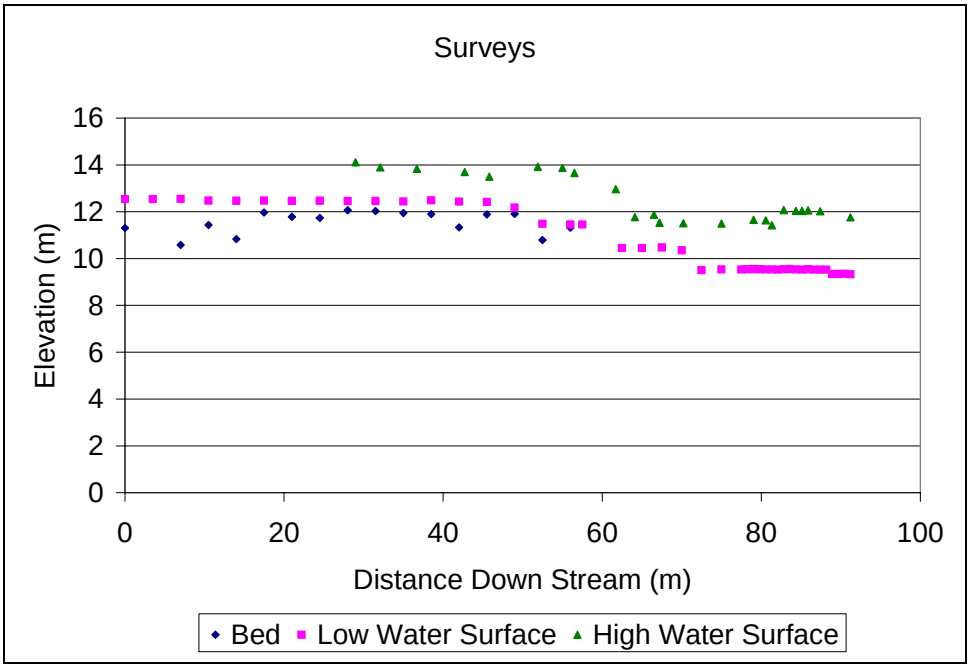

Figure 10 Bed, Low Water Surface, and High Water Surface Profiles. Bedrock 0-15 m, particle jam 15-60 m, bedrock 60-80 m, gravel/cobble 80-91 m.

iv. Channel width, effective width, and unit stream power versus distance downstream

Channel width varied more than any other dependent variable. Width was constricted the most at the knickpoint. Also, the cross sections show that above the knickpoint there were two areas of width constriction which was followed by large recirculation eddies that formed once the width expanded. These eddies deposited a great deal of sand, which was the suspended sediment in that reach.

The difference between width and effective width is very important within this reach. The upper section featured a series of three steps, which slowed down the flow, thus creating recirculation eddies and forcing the majority of the flow toward the western banks. This made

the area above the knickpoint very narrow in regard to the actual space the flow had available to move (see figure 11). The recirculation eddies also carved out the area where the next particle jam could originate from (see figure 12).

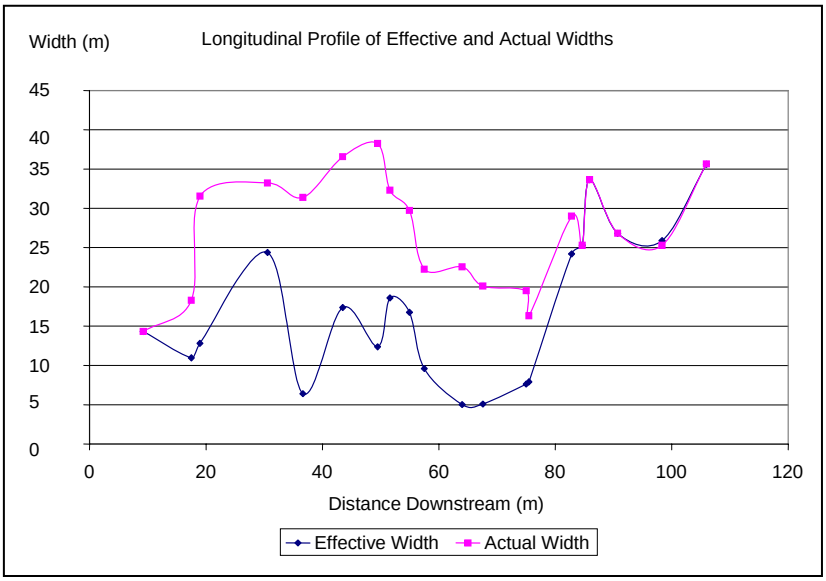

Figure 11 Longitudinal Profile of Width and Effective Width. Bedrock 0-15 m, particle jam 15-60 m, bedrock 60-80 m, gravel/cobble 80-91 m.

Figure 12 Picture of Sand deposit of April 22nd, 2006 flood. Sand is the suspended sediment deposited in this recirculation eddy.

From the channel width and the effective width, stream power per unit width can be calculated. This can be plotted longitudinally to compare unit stream power to morphology (see

figure 13). Above the boulder knickpoint stream power is fairly high and decreases as the water moves over the knickpoints. After passing the knickpoints, unit stream power remains fairly constant. The fact that stream power decreases just above and over the knickpoints lead to the assumption that the boulder knickpoint is very stable. If the stream power per unit width was very high over that area, then the boulders would be swept away and the feature would not exist.

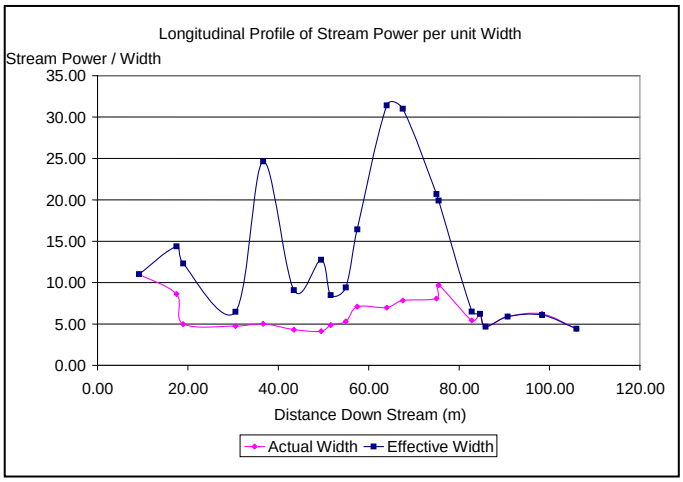

Figure 13 Stream power per unit width. Bedrock 0-15 m, particle jam 15-60 m, bedrock 60-80 m, gravel/cobble 80-91 m.

v. Stability of channel bed

The affects of shear stress within this reach explain why the particle jam has remained. At the particle jam, there is not enough energy available to move the particles from that location. So once the particles get stuck, there is no way to move them. With the particle jam being such a solid structure in the stream, the affects of it become clearer. The particle jam could act as both a strainer of particles, to keep the bedrock clear in order to keep the bedrock abrasion going and also as a funnel of flow. At the particle jam there are many boulders that are suck due to the width constriction in that area. The flow is dictated by the width constriction and the particle

organization. During low flow, the particle jam splits the flow into two parts, the western flow moving much more steady and straight than the eastern flow. This forms a mixing of turbulence when those two flows meet. The chaos in turbulence causes more energy to be expended, and the water moves over the last part of the bedrock knickpoint in the smallest of flows, with less force as what might be expected.

a. Above boulder knickpoint

Using the bed and water surface profiles for the upper reach, mid channel depth can be obtained (see figure 14). This can be plotted as a function of distance a shows a similar pattern to that of width and effective width plotted as a function of distance (see figures 13 and 14). With depth and slope, a shear stress may be calculated and plotted against distance downstream (see figure 15). Above the knickpoint, D50 was approximately 0.40 meters and the D84 was approximately 2.24 meters. All of the particles were orientated with their longest axis parallel to the flow direction. This suggests that the particles rest in that place long enough to get orientated is such a way. These particles also mix with large pieces of bedrock which remained in the stream. With the knowledge of D50 and D84 dimensionless shear stress longitudinally shows that the particles above the reach are no where close to the possibility of getting moved, considering that the value to move gravel in a cobble bedded stream is 0.045 (Wiberg 1991).

Distance	Mid Depth	Shear	T*	T*
(m)	(m)		0.4 m	2.24 m
0	3.78	631.91	0.098	0.017
3.5				
7	4.33	725.22	0.112	0.020
10.5	3.40	569.39	0.088	0.016
14	3.92	656.21	0.101	0.018
17.5	2.71	453.51	0.070	0.013

21	2.81	470.05	0.073	0.013
24.5	2.78	464.83	0.072	0.013
28	2.37	396.01	0.061	0.011
29				
31.5	2.32	387.44	0.060	0.011
32.1				
35	2.32	388.58	0.060	0.011
36.7				
38.5	2.28	382.02	0.059	0.011
42	2.77	463.82	0.072	0.013
42.7				
45.5	2.14	358.19	0.055	0.010
45.8				
49	2.03	340.42	0.053	0.009
51.9				
52.5	3.07	513.42	0.079	0.014
55				
56	2.46	411.98	0.064	0.011
56.5	2.72	454.72	0.070	0.013

Figure 14 Upper Reach Shear Stress

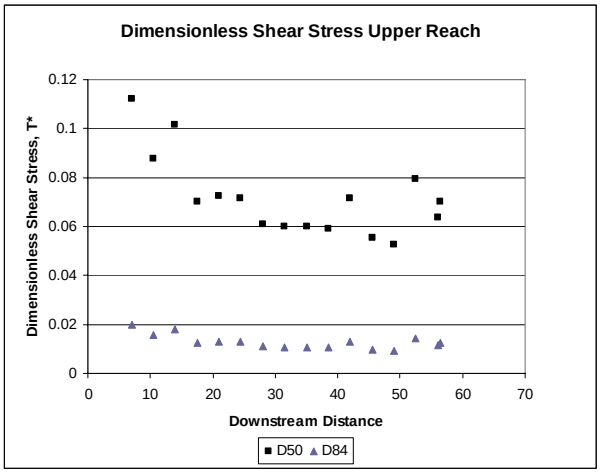

Figure 15 Upper Reach Dimensionless Shear Stress. Bedrock 0-15 m, particle jam 15-60 m, bedrock 60-80 m, gravel/cobble 80-91 m.

b. Below boulder knickpoint

The mobility of sediment in the lower reach is shown as a function of mobility in a cross section. By doing this, localized shear stresses can be evaluated and used to determine if the

majority of the bed particles can be moved. The D50 of the lower reach was approximately 0.26 meters and the D84 approximately 0.56 meters. The particles in this section had a more random orientation. Approximately 50% of the particles had their long axis parallel to the flow while the other 50% had a different orientation in the stream. The randomness in the orientations suggest that the particles do not remain in the cross section long enough to acquire the typical long axis parallel to stream flow. This section was much more alluvial and contained much less bedrock intrusion. The only large particles present in the section were on the rim of the plunge pool. These may be relics of a past particle jams failing. The shear stress and dimensionless shear stress demonstrate that the gravel in this section moves readily (see figures 16 and 17).

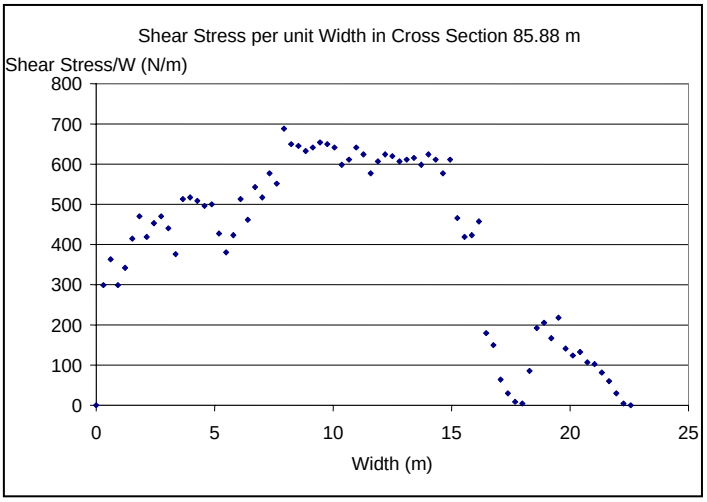

Figure 16 Shear Stress at 85.88 meter cross section

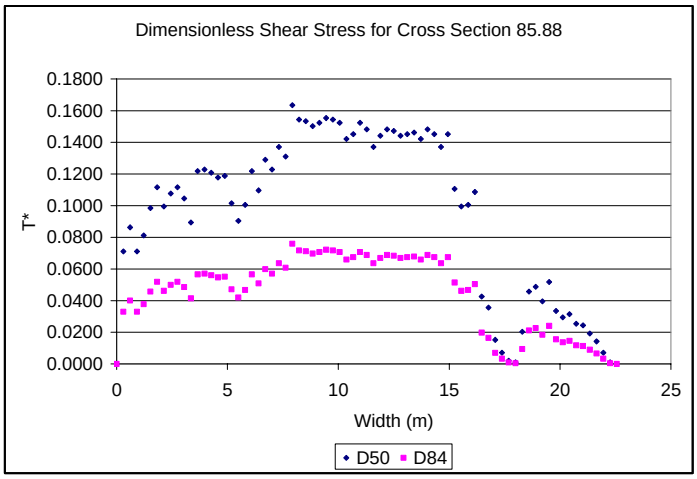

Figure 17 Dimensionless Shear Stress for Cross Section 85.88 m

VI. Discussion

The most important hydraulic feature turned out to be the boulder knickpoint instead of the bedrock knickpoint. The boulder knickpoint caused the flow during a flood to plunge and become supercritical. When this happened, a hydraulic jump occurred just downstream of the boulder knickpoint as the flow went from supercritical to subcritical. From the calculations of stream power and shear stress, it is possible to explain why the boulder knickpoint has sustained itself: the widths and depths proceeding the feature force stream power low and shear stress can know become large enough to move the largest of particles when anchor down the knickpoint. The boulder knickpoint also strained out the particles which would usually fall in place on the bedrock knickpoint, thus keeping the bedrock clear for abrasion. Bedrock knickpoints migrate by having a boulder knickpoint above it which functions as a shield for settling particles. Boulder knickpoints migrate by backing up the larger particles above it, which begin to form a new place for the particle jam, at an area in the stream which has a width constriction. The bedrock abrasion undermines the boulder knickpoint, eventually releasing its width constriction, leaving

features such as a hydraulic arc behind. As it turns out, particle distribution on a local scale has become the most important parameter within this study.

VII. Suggestions for Future Work

The intensive study of the morphology and hydraulics of one knickpoint on Northwest Branch of the Anacostia River have lead to many insights as far as how a particle jam is able to sustain itself and why it accumulates where it does. The next logical step for this research would be to go to other knickpoints in this region to see if similar morphological characteristics exist and if they can be explained by the processes explained here. Another area of research would be to see how these hydraulic conditions affect migration speed. This links the placement of the knickpoint to the tectonic history of the area. If there are large enough affects by the hydraulics of the area, then the location of a knickpoint is not indicative of just past sea water levels.

Another area of future research would be into how else particle distributions affect certain hydraulic conditions. Bedrock/Boulder bed streams may not be the only streams where there is such a large of affect simply by the orientation and distribution of the sediment.

VIII. Acknowledgements

My project could not have gotten to this stage without the continual support from my advisor, Dr. Karen Prestegaard. She has helped develop this project from the beginning and has been there for all of my questions. Out in the field, I also have to thank Joshua Long and Daniel Liden for help with cross-sections, pictures, and surveying. Also Dr. Prestegaard's

Geomorphology 2006 class helped gather crucial last minute data on flood and effective widths. For data processing, Joshua Long has helped in compiling and graphing some suites of data and has been the go to person to bounce ideas off of. I appreciate the consultation with Dr. En-Zen and the continuing guidance through 393 and 394 Phil Candela.

IX. References

Boyd, W. (1928). A new method of determining the rate of recession of Niagara Falls. *Proceedings and transactions of the Royal Society of Canada*, 22

Canavan, W. (1989). The Fluvial Geomorphology of a Northern Appalachian bedrock stream, New Haven River, central Vermont. *Master's Thesis Southern Illinois University*.

Cazeau, C. & Calkins, P. (1965). Buffalo and Niagara Falls. *In Guidebook for Field Conference A, New England-New York State--Internat. Assoc. Quaternary Research, 7th Cong., \U.S.A., 1965.*

Chin, A. (1999) The morphologic structure of step-pools in mountain streams. *Geomorphology*, 27, 191-204.

Clancy, Katherine Ann. (2003). Methods to measure and analyze particle organization in boulder-bed streams. Doctorate *Thesis University of Maryland College Park*.

Fleeger, G., Braun, D., & Inners, J. (2002). Plunge into the past or go with the flow; multiple hypotheses for the origin of the Archbald Pothole, Lackawanna County, Pennsylvania. *Abstracts with Programs- Geological Society of America*. 34(1), 27-.

Frankel, K., Vaughn, J., & Pazzaglia, F. (2001). Knickpoint retreat and long profile evolution through a vertically bedded substrate; a flume study. *Abstracts with programs - Geological Society of America*, 33(6), 314-.

Hancock, G., Anderson, R., & Whipple, K. (2000). Beyond Power: Bedrock river incision process and form. *Rivers Over Rock: Fluvial Processes in Bedrock Channels*, Geophysical Monograph 107.

Hayakawa, Y. & Matsukura, Y. (2003) Recession rates of waterfalls in Boso Peninsula, Japan, and a predictive equation. Earth surface processes and landforms, 28(6)

Johnson, J. & Whipple, K. (2004). Expirmental Bedrock Channel Incision: Scaling, Sculpting, and Sediment Transport. *Eos Tras AGU*, 85(47).

Madeji, M.A., (2003). Rivers on rocks; the influence of geology on fluvial processes and landforms. *Abstracts with Programs - Geological Society of America*, 35(6), 351-.

Pasternack, G. (2004). Mechanics of Horseshoe Waterfalls. *Eos Tras AGU*, 85(47).

Phillips, W. (2003). Rates of knickpoint migration and bedrock erosion from cosmogenic Be-10 in a landscape of active normal faulting. *Abstracts with programs - Geological Society of America*, 35(6), 63-.

Reichmuth, D.R,. (2005) Floodplain Management Short Course prepared by FEMA.

Schmidt, M. (1993) Maryland's Geology. Tidewater Publishers.

Schoenbohm, L. (2001). Recent deformation along the Red River Fault as constrained by river incision into a low relief relict landscape, Yunnan, China. Abstracts *with programs - Geological Society of America*, 33(6), 258-.

Spencer, J. (1908). Recession of the Niagara Falls. *Report - British Association for the Advancement of Science*.

Spencer, J. (1898). Niagara as a timepiece. *Proceedings of the Canadian Institute*.

Springer, G. (2004). Inner channel development and knickpoint retreat in an anabranching river by potholing. Abstracts *with programs - Geological Society of America*, 36(5)

Whipple, K. (2000). River incision into bedrock; mechanics and relative efficacy of plucking, abrasion, and cavitation. *Geological Society of America bulletin*, 112(3).

Wiberg, P and Smith, J. Dungan (1991). Velocity Distribution and Bed Roughness in High-Gradient Streams. *Water Resources Research*, 27(5).

Wohl, E., & Achyuthan, H. (2002). Substrate influences on incised-channel morphology. *The Journal of Geology*, 110, 115-120.

Wohl, E., & Ikeda, H. (1998). Patterns of bedrock channel erosion on the Boso Peninsula, Japan. *The Journal of Geology*, 106, 331-345.

Zimmermann, A., & Church, M. (2001). Channel Morphology, gradient profiles and bed stresses during flood in a step-pool channel. *Geomorphology*, 40, 311-327.

Appendix 1: Flood Data

Hyattsville Gauging Station

peak_dt	peak_va	gage_ht	Rank	RI	Q/A
	cfs	ft			
10d	8s	8s			
6/22/1972	18000	14.47	1	52	364.37247
9/26/1975	14800	11.17	2	26	299.595142
9/6/1979	12000	9.4	3	17.33333	242.91498
7/27/2004	9310	8.24	4	13	188.461538
9/23/2003	7230	7.24	5	10.4	146.356275
9/14/1966	7000	13.5	6	8.666667	141.700405
8/10/1969	6050	13.2	7	7.428571	122.469636
9/16/1976	5540	6.59	8	6.5	112.145749
8/25/1967	5030	12.67	9	5.777778	101.821862
9/16/1999	4570	5.77	10	5.2	92.5101215
1/26/1978	4440	5.91	11	4.727273	89.8785425
8/8/1959	4170	12.12	12	4.333333	84.4129555
10/1/1979	3780	5.27	13	4	76.5182186
10/25/1976	3620	5.36	14	3.714286	73.2793522
7/22/1958	3590	11.67	15	3.466667	72.6720648
9/1/1952	3360	11.4	16	3.25	68.0161943
7/9/1970	3220	10.53	17	3.058824	65.1821862
8/20/1973	3200	6.63	18	2.888889	64.7773279
8/20/1963	3200	11	19	2.736842	64.7773279
8/4/1960	3180	11.31	20	2.6	64.3724696
8/23/2001	3010	4.77	21	2.47619	60.9311741
10/14/1955	3010	11.32	22	2.363636	60.9311741
6/15/1954	2980	10.69	23	2.26087	60.3238866
8/22/1955	2930	11.19	24	2.166667	59.3117409
11/22/1952	2710	10.16	25	2.08	54.8582996
3/30/1974	2640	6.22	26	2	53.4412955
8/27/1971	2510	9.12	27	1.925926	50.8097166
5/28/1982	2470	4.34	28	1.857143	50
3/5/1965	2390	9.82	29	1.793103	48.3805668
7/27/1945	2300	10.02	30	1.733333	46.5587045
9/10/1950	2280	9.86	31	1.677419	46.1538462
10/16/1942	2280	9.92	32	1.625	46.1538462
4/15/1983	2230	4.14	33	1.575758	45.1417004
4/13/1961	2210	9.68	34	1.529412	44.7368421
8/9/1942	2180	9.52	35	1.485714	44.1295547
8/27/2000	2150	4.1	36	1.444444	43.5222672
6/13/1951	2130	9.03	37	1.405405	43.1174089
6/14/1981	2060	4	38	1.368421	41.7004049
11/9/1943	2000	8.82	39	1.333333	40.48583

1/14/1968	1900	8.38	40	1.3	38.4615385
8/3/1948	1900	8.37	41	1.268293	38.4615385
4/26/1939	1880	6.03	42	1.238095	38.0566802
5/31/1962	1810	8.82	43	1.209302	36.6396761
4/20/1940	1750	6.48	44	1.181818	35.4251012
9/1/2002	1710	3.68	45	1.155556	34.6153846
11/6/1963	1700	8.6	46	1.130435	34.4129555
5/23/1949	1650	7.48	47	1.106383	33.4008097
6/5/1957	1550	9.16	48	1.083333	31.3765182
9/6/1947	1300	6.37	49	1.061224	26.3157895
6/29/1946	1300	6.41	50	1.04	26.3157895
7/13/1941	1050	5.11	51	1.019608	21.2550607

Colesville Gauging Station

peak_dt	peak_va	gage_ht	Rank	RI	
	cfs	ft			
10d	8s	8s			
6/22/1972	11000	15.89	1	52	521.327
7/15/1975	6640	12.24	2	26	314.6919
9/5/1979	6300	11.47	3	17.33333	298.5782
8/8/1953	4910	10.99	4	13	232.7014
9/1/1952	4110	9.74	5	10.4	194.7867
11/25/1950	3960	9.7	6	8.666667	187.6777
9/23/2003	2720	9.92	7	7.428571	128.91
6/23/2001	2410	9.65	8	6.5	114.218
8/4/1971	2240	9.87	9	5.777778	106.1611
9/14/1966	2100	9.57	10	5.2	99.52607
9/16/1999	2070	9.32	11	4.727273	98.10427
5/23/1949	2030	8.8	12	4.333333	96.20853
7/27/1945	2020	8.37	13	4	95.7346
1/26/1978	1960	9.36	14	3.714286	92.891
8/25/1967	1740	9.15	15	3.466667	82.46445
7/21/1956	1550	8.86	16	3.25	73.45972
1/1/1976	1480	8.75	17	3.058824	70.14218
8/13/1955	1470	8.73	18	2.888889	69.66825
3/21/1998	1420	8.08	19	2.736842	67.29858
4/14/1970	1380	8.56	20	2.6	65.40284
11/8/1943	1320	7.37	21	2.47619	62.55924
5/28/1946	1320	7.33	22	2.363636	62.55924
7/9/1958	1290	8.34	23	2.26087	61.13744
4/15/1983	1250	8.21	24	2.166667	59.24171
9/10/1950	1240	7.75	25	2.08	58.76777
3/30/1974	1230	8.21	26	2	58.29384
3/5/1965	1210	8.14	27	1.925926	57.34597
1/1/1948	1190	7.1	28	1.857143	56.3981
10/1/1979	1190	8.08	29	1.793103	56.3981

5/12/1943	1160	7.06	30	1.733333	54.9763
8/10/1969	1100	7.82	31	1.677419	52.1327
6/5/1963	1080	7.83	32	1.625	51.18483
4/13/1961	1060	7.75	33	1.575758	50.23697
6/5/1957	941	7.37	34	1.529412	44.59716
8/8/1959	941	7.37	35	1.485714	44.59716
1/14/1968	935	7.26	36	1.444444	44.3128
12/8/1972	900	7.12	37	1.405405	42.65403
2/19/1960	842	7.01	38	1.368421	39.90521
8/3/2002	821	6.13	39	1.333333	38.90995
1/9/1964	814	6.77	40	1.3	38.5782
3/12/1962	798	6.79	41	1.268293	37.81991
3/21/2000	795	6.01	42	1.238095	37.67773
4/28/1954	772	6.66	43	1.209302	36.58768
4/8/1940	730	5.82	44	1.181818	34.59716
2/3/1982	722	6.41	45	1.155556	34.21801
1/30/1939	680	5.6	46	1.130435	32.22749
11/27/1940	680	5.36	47	1.106383	32.22749
7/4/1981	599	5.62	48	1.083333	28.38863
3/22/1977	588	5.58	49	1.061224	27.8673
9/7/1947	500	4.53	50	1.04	23.69668
8/11/1942	430	4.21	51	1.019608	20.37915

Appendix 2: Cross Sections

At 64 meters

Distance		Channel Depth	Water Depth
(ft)	(m)	(m)	(m)
0	0	0	
1	0.30	-0.7	
2	0.61	-0.85	
3	0.91	-0.7	
4	1.22	-0.8	
5	1.52	-0.97	
6	1.83	-1.1	
7	2.13	-0.98	
8	2.44	-1.06	
9	2.74	-1.1	
10	3.05	-1.03	
11	3.35	-0.88	
12	3.66	-1.2	
13	3.96	-1.21	
14	4.27	-1.19	
15	4.57	-1.16	
16	4.88	-1.17	
17	5.18	-1	
18	5.49	-0.89	
19	5.79	-0.99	
20	6.10	-1.2	
21	6.40	-1.08	
22	6.71	-1.27	
23	7.01	-1.21	
24	7.32	-1.35	-1.35
25	7.62	-1.29	-1.29
26	7.93	-1.61	-1.46
27	8.23	-1.52	-1.45
28	8.54	-1.51	-1.42
29	8.84	-1.48	-1.41
30	9.15	-1.5	-1.4
31	9.45	-1.53	-1.38
32	9.76	-1.52	-1.35
33	10.06	-1.5	-1.35
34	10.37	-1.4	-1.33
35	10.67	-1.43	-1.31
36	10.98	-1.5	-1.28
37	11.28	-1.46	-1.3
38	11.59	-1.35	-1.29
39	11.89	-1.42	-1.3
40	12.20	-1.46	-1.34

41	12.50	-1.45	-1.38
42	12.80	-1.42	-1.35
43	13.11	-1.43	-1.33
44	13.41	-1.44	-1.33
45	13.72	-1.4	-1.31
46	14.02	-1.46	-1.3
47	14.33	-1.43	-1.3
48	14.63	-1.35	-1.3
49	14.94	-1.43	-1.3
50	15.24	-1.09	-1.09
51	15.55	-0.98	
52	15.85	-0.99	
53	16.16	-1.07	
54	16.46	-0.42	
55	16.77	-0.35	
56	17.07	-0.15	
57	17.38	-0.07	
58	17.68	-0.02	
59	17.99	-0.01	
60	18.29	-0.2	
61	18.60	-0.45	
62	18.90	-0.48	
63	19.21	-0.39	
64	19.51	-0.51	
65	19.82	-0.33	
66	20.12	-0.29	
67	20.43	-0.31	
68	20.73	-0.25	
69	21.04	-0.24	
70	21.34	-0.19	
71	21.65	-0.14	
72	21.95	-0.07	
73	22.26	-0.01	
74	22.56	0	

At 82.8 meters

Distance		**Bed**
(ft)	**(m)**	**(m)**
0	0.0	0
1	0.3	0.1
2	0.6	0.35
3	0.9	0.5
4	1.2	0.67
5	1.5	0.55

6	1.8	0.69
7	2.1	1.15
8	2.4	1.275
9	2.7	0.835
10	3.0	0.83
11	3.4	0.9
12	3.7	1.685
13	4.0	1.6
14	4.3	1.635
15	4.6	1.64
16	4.9	1.8
17	5.2	1.82
18	5.5	1.83
19	5.8	1.8
20	6.1	1.875
21	6.4	1.87
22	6.7	1.97
23	7.0	1.56
24	7.3	2.455
25	7.6	2.31
26	7.9	2.49
27	8.2	2.44
28	8.5	2.3
29	8.8	2.31
30	9.1	2.58
31	9.4	2.6
32	9.8	2.63
33	10.1	2.68
34	10.4	2.74
35	10.7	2.61
36	11.0	2.7
37	11.3	2.73
38	11.6	2.76
39	11.9	2.8
40	12.2	2.57
41	12.5	2.55
42	12.8	2.73
43	13.1	2.68
44	13.4	2.76
45	13.7	2.69
46	14.0	2.68
47	14.3	2.58
48	14.6	2.44
49	14.9	2.41
50	15.2	2.41
51	15.5	2.3
52	15.8	2.35
53	16.2	2.24

54	16.5	2.32
55	16.8	2.4
56	17.1	2.35
57	17.4	2.39
58	17.7	2.35
59	18.0	2.39
60	18.3	2.44
61	18.6	2.49
62	18.9	2.28
63	19.2	2.45
64	19.5	2.3
65	19.8	2.09
66	20.1	1.95
67	20.4	1.94
68	20.7	2.03
69	21.0	1.97
70	21.3	1.91
71	21.6	1.88
72	21.9	1.67
73	22.3	1.67
74	22.6	1.63
75	22.9	1.61
76	23.2	1.57
77	23.5	1.38
78	23.8	1.4
79	24.1	1.35
80	24.4	1.3
81	24.7	1.27
82	25.0	1.21
83	25.3	1.19
84	25.6	1.13
85	25.9	1.2
86	26.2	0.89
87	26.5	0.8
88	26.8	0.54
89	27.1	0.69
90	27.4	0.55
91	27.7	0.49
92	28.0	0.44
93	28.3	0.32
94	28.7	0.14
95	29.0	0

At 17.5 meters

Distance (ft)	Depth (m)
0	0
1	0.13
2	0.15
3	0.17
4	0.23
5	0.28
6	0.32
7	0.36
8	0.27
9	0.52
10	0.58
11	0.7
12	0.49
13	0.5
14	1.12
15	1.02
16	0.61
17	0.71
18	0.97
19	1.36
20	1.3
21	1.09
22	1.14
23	1.13
24	1.13
25	1.17
26	1.24
27	1.34
28	1.32
29	1.32
30	1.33
31	1.32
32	1.22
33	1.195
34	1.14
35	1.06
36	0.91
37	0.87
38	0.785
39	0.745
40	0.71
41	0.66
42	0.675
43	0.71

44	0.7
45	0.69
46	0.66
47	0.625
48	0.6
49	0.55
50	0.595
51	0.7
52	0.73
53	0.59
54	0.57
55	0.5
56	0.43
57	0.395
58	0.32
59	0.21
60	0

At 70 meters

Distance (ft)	Depth (m)
-1	0
0	1.618
1	1.704
2	1.718
3	1.752
4	1.774
5	2
6	1.865
7	1.7
8	1.65
9	2.109
10	2.134
11	2.175
13	2.092
14	2.038
15	1.945
16	1.882
17	1.83
18	1.96
19	2.525
20	2.325
21	2.45
22	2.41
23	2.51

24	3.406
25	3.419
26	3.532
27	3.575
28	3.52
29	3.425
30	3.325
31	2.305
32	2.297
33	2.291
34	2.345
35	2.45
36	2.595
37	2.72
38	2.85
39	3.025
40	3.565
41	3.72
42	3.67
43	3.69
44	3.5
45	3.54
46	3.69
47	3.72
48	3.528
49	3.555
50	3.705
51	3.69
52	3.752
53	3.78
54	3.7
55	3.68
56	3.118
57	3.215
58	3.162
59	3.279
60	2.625
61	3.2
62	3.06
63	2.735
66	0

At 85.88 meters

distance (m)	depth (m)
0	0
1	0.8
2	1.4
3	1.6
4	1.95
5	2.4
6	2.2
7	2.05
8	1.9
9	1.7
10	2.2
11	1.7
12	1.7
13	2
14	2.15
15	2.7
16	2.9
18	2.55
19	1.9
20	1.4
21	1.4
22	1.65
23	1.2
24	1.93
25	1.7
26	1.5
27	2
30	1.8
31	0.3
32	0.1
33	0.1
33.65	0

Graph at 64 meters

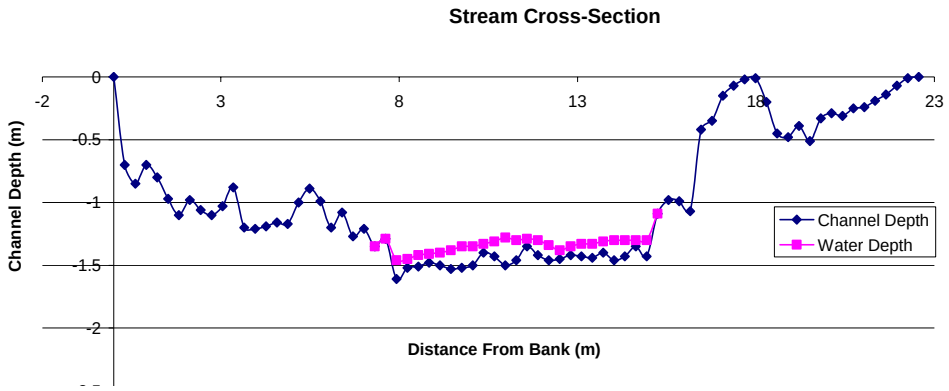

Graph at 82.88

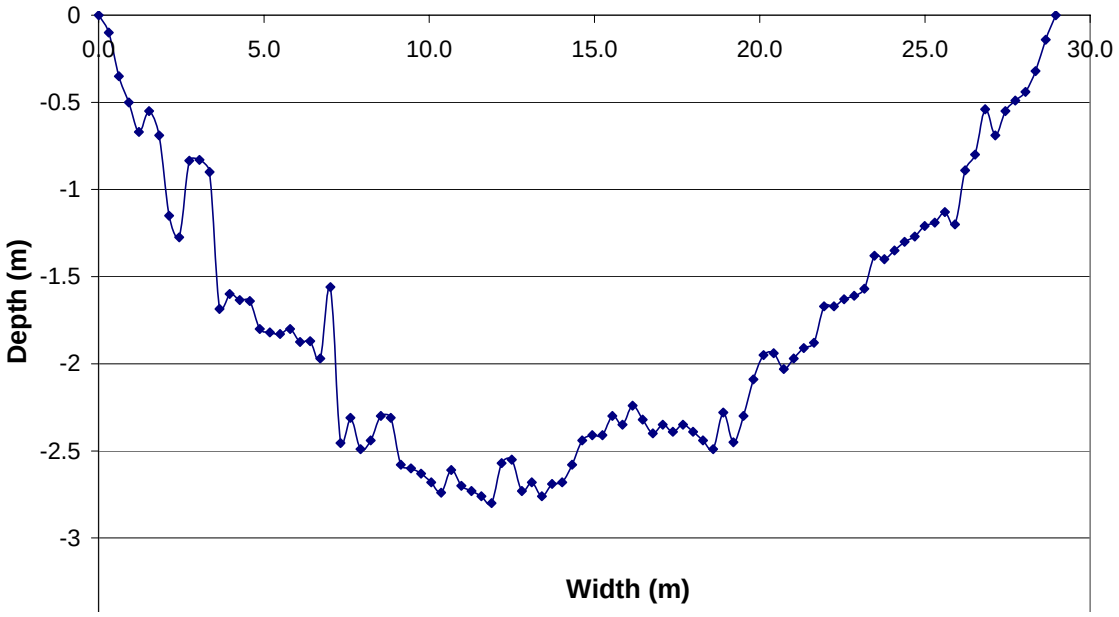

Graph at 17.5 meters

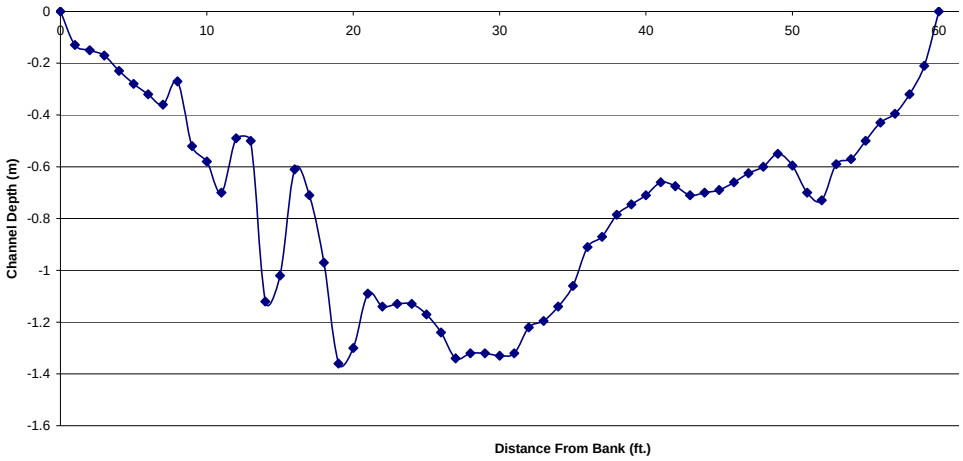

Graph at 75 meters

Cross Section 3

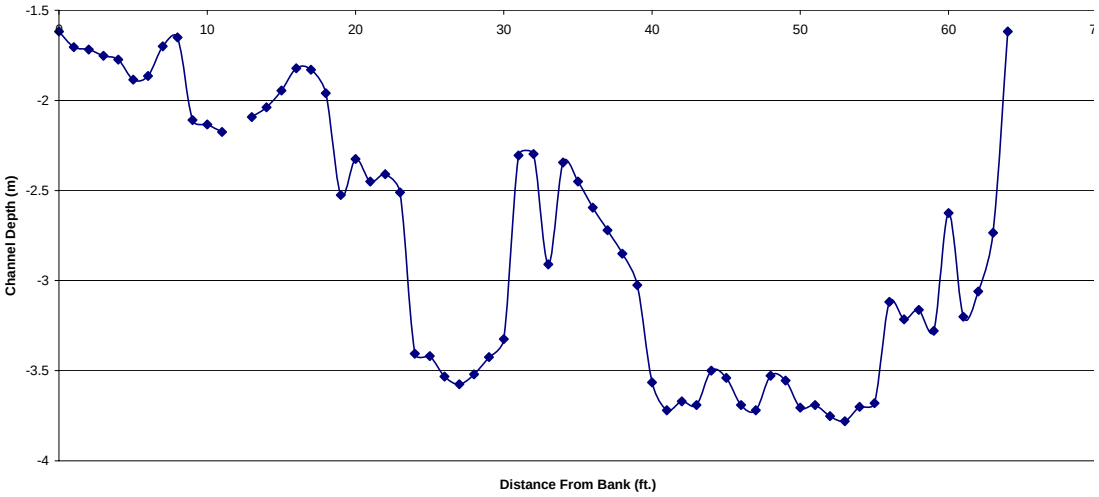

Graph at 85.88 meters

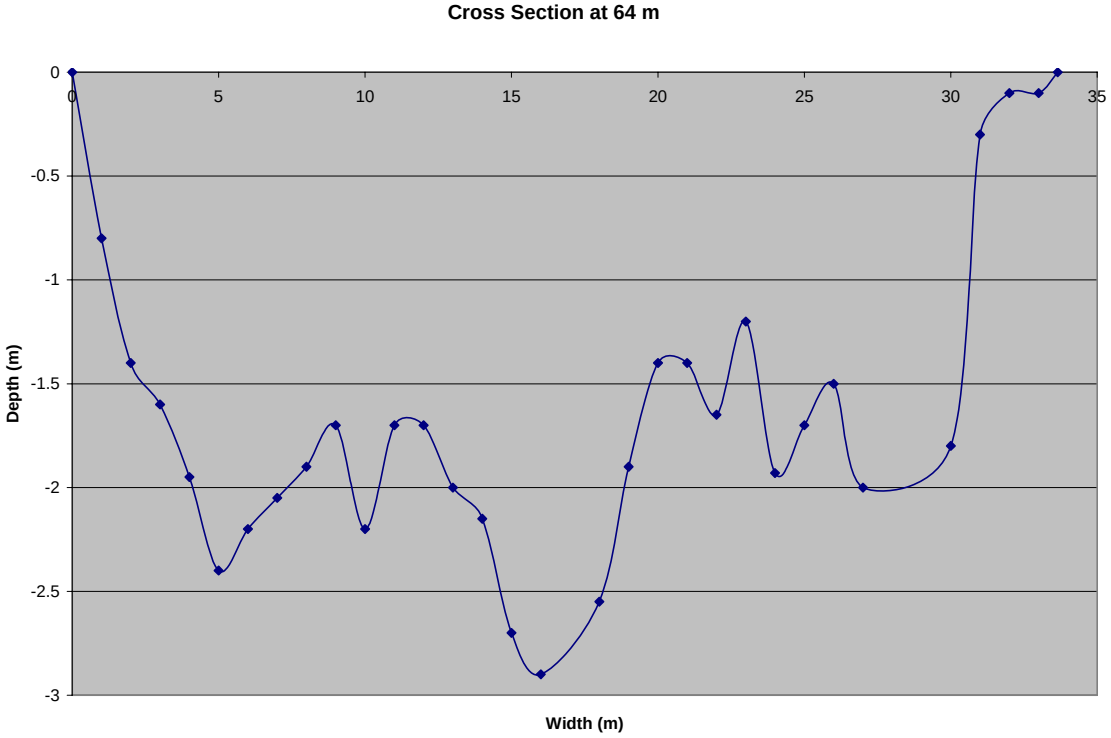
Cross Section at 64 m
0
-0.5
-1
-1.5
-2
-2.5
-3
Depth (m)
0
5
10
15
20
25
30
35
Width (m)

Appendix 3: Bed and Water Surface Profiles

Surveyed Data

Distance (m)	Bed (m)	Low (m)	High (m)
0	11.302	12.537	
3.5		12.542	
7	10.582	12.547	
10.5	11.432	12.477	14.627
14	10.832	12.472	
17.5	11.962	12.477	
21	11.782	12.462	
24.5	11.732	12.467	
28	12.062	12.457	
29			14.052
31.5	12.032	12.452	
32.1			14.33
35	11.944	12.437	
36.7			14.226
38.5	11.902	12.480	
42	11.332	12.432	
42.7			14.085
45.5	11.882	12.417	
45.8			
49	11.907	12.177	
51.9			13.87
52.5	10.792	11.482	
55			13.8
56	11.317	11.452	
56.5	11.05		13.656
57.500		11.452	
61.700			12.969
62.500		10.450	
64.100			11.766
65.000		10.452	
66.500			11.869
67.200			11.532
67.500		10.472	
70.000		10.347	
70.200			11.509
72.500		9.504	
75.000		9.534	11.492
77.500		9.537	
78.262		9.545	
79.024		9.547	11.653
79.786		9.545	
80.548		9.533	11.635

81.310		9.538	11.423
82.072		9.531	
82.834		9.539	12.074
83.596		9.546	
84.358		9.536	12.039
85.120		9.527	12.039
85.882		9.541	12.057
86.644		9.525	
87.406		9.527	12.025
88.168		9.525	
88.930		9.332	
89.692		9.341	
90.454		9.345	
91.216		9.325	11.765

Graph

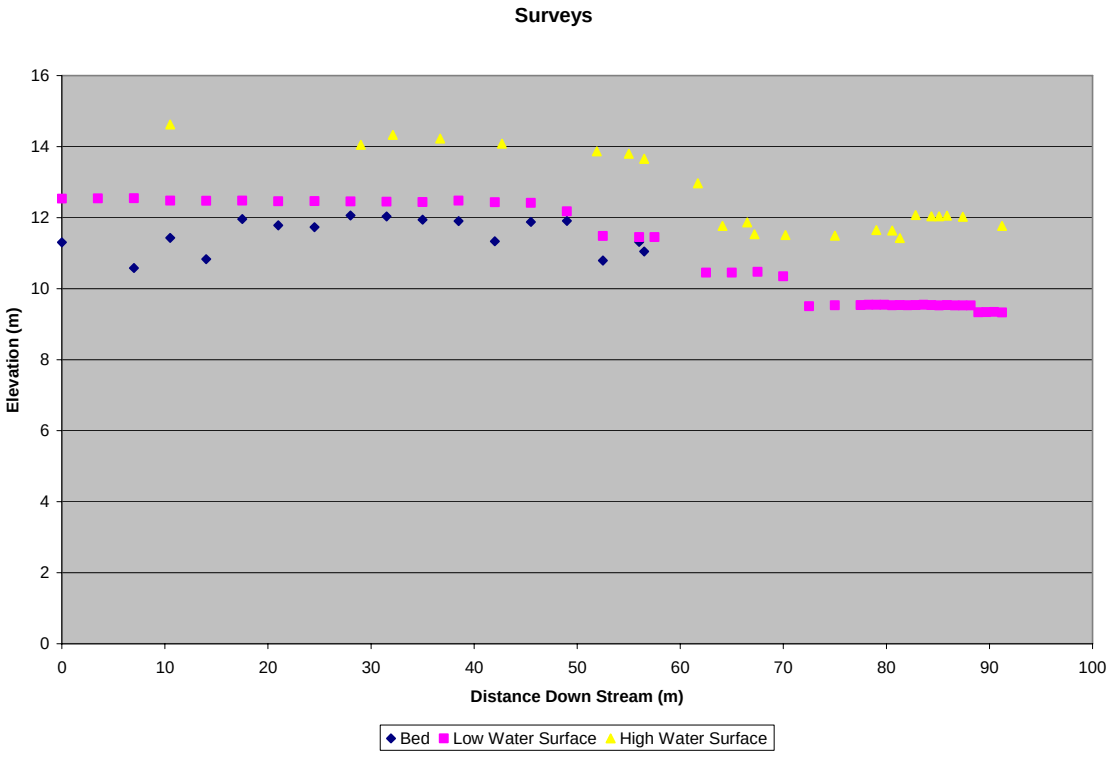

Appendix 4: Shear Stress and Grain Size Distributions

Upper Reach

Distance	Mid Depth	Shear	T*	T*
(m)	(m)		0.4 m	2.24 m
0	3.78	631.91	0.098	0.017
3.5				
7	4.33	725.22	0.112	0.020
10.5	3.40	569.39	0.088	0.016
14	3.92	656.21	0.101	0.018
17.5	2.71	453.51	0.070	0.013
21	2.81	470.05	0.073	0.013
24.5	2.78	464.83	0.072	0.013
28	2.37	396.01	0.061	0.011
29				
31.5	2.32	387.44	0.060	0.011
32.1				
35	2.32	388.58	0.060	0.011
36.7				
38.5	2.28	382.02	0.059	0.011
42	2.77	463.82	0.072	0.013
42.7				
45.5	2.14	358.19	0.055	0.010
45.8				
49	2.03	340.42	0.053	0.009
51.9				
52.5	3.07	513.42	0.079	0.014
55				
56	2.46	411.98	0.064	0.011
56.5	2.72	454.72	0.070	0.013

	at	71.73	meters
Order	A	B	//
	(cm)	(cm)	
1.00	20.00	15.00	A
2.00	18.00	13.00	A
3.00	10.00	10.00	A
4.00	17.00	10.00	A
5.00	33.00	20.00	A
6.00	33.00	18.00	A
7.00	9.50	4.00	A
8.00	14.00	9.00	A
9.00	10.00	6.00	A
10.00	15.00	14.00	B
11.00	24.00	23.00	B

12.00	22.00	10.00	A
13.00	17.00	14.50	A
14.00	14.50	9.00	A
15.00	7.00	2.50	B
16.00	8.00	7.00	A
17.00	10.00	7.00	A
18.00	6.00	5.00	A
19.00	4.50	3.50	A
20.00	2.00	1.50	A
21.00	7.00	4.50	A
22.00	2.00	1.00	A
23.00	1.00	0.50	A
24.00	3.50	1.50	A
25.00	4.00	3.00	A
26.00	5.00	3.00	B
27.00	10.00	7.00	A
28.00	5.00	4.50	A
29.00	9.00	5.00	B
30.00	4.50	3.00	B
31.00	3.00	2.00	A
32.00	7.00	5.00	A
33.00	5.00	5.00	A
34.00	50.00	30.00	A
35.00	50.00	29.00	B
36.00	36.00	16.00	B
37.00	33.00	27.00	A
38.00	64.00	45.00	A
39.00	4.00	2.00	A
40.00	9.00	4.00	A
41.00	16.00	9.00	A
42.00	40.00	20.00	A
43.00	44.00	40.00	A
44.00	77.00	57.00	A
45.00	150.00	40.00	A
46.00	2.00	1.00	A
47.00	12.00	7.00	A
48.00	100.00	72.00	A
49.00	45.00	33.00	A
50.00	3.50	2.50	A
51.00	2.50	1.50	A
52.00	3.50	2.00	A
53.00	160.00	140.00	A
54.00	160.00	144.00	A

at	26.00	meters
A	B	//
(cm)	(cm)	

100.00	60.00	A
46.00	30.00	A
30.00	15.00	A
15.00	10.00	A
9.00	9.00	A
340.00	260.00	A
8.00	2.00	A
115.00	65.00	A
130.00	75.00	A
134.00	45.00	A
422.00	100.00	A
234.00	132.00	A
456.00	340.00	A
22.00	13.00	A
335.00	278.00	A
223.00	201.00	A
33.00	27.00	A
478.00	355.00	A
236.00	132.00	A
234.00	184.00	A
332.00	233.00	A
113.00	86.00	A
135.00	95.00	A
185.00	142.00	A
135.00	93.00	A
12.00	5.00	A
1.00	0.50	A
224.00	223.00	A

at	56.48	meters
A	B	//
(cm)	(cm)	
40.00	20.00	A
10.00	7.00	A
7.00	3.00	A
12.00	5.00	A
4.00	2.50	A
4.00	3.50	A
95.00	26.00	A
14.00	7.00	A
66.00	45.00	A
97.00	58.00	A
62.00	46.00	A
100.00	62.00	A
143.00	80.00	A
127.00	60.00	A
398.00	253.00	A

320.00	245.00	A
31.00	12.00	A
224.00	178.00	A
122.00	94.00	A
248.00	176.00	A
128.00	104.00	A
309.00	274.00	A
228.00	147.00	A
240.00	186.00	A
128.00	87.00	A
328.00	264.00	A
231.00	103.00	A
213.00	159.00	A
119.00	79.00	A
123.00	93.00	A
221.00	168.00	A
224.00	176.00	A

A	B	Order	Distribution	Percentage
Size, cm	Size, cm		Frequency	
1.00	0.50	1.00	0.02	1.69
1.00	0.50	2.00	0.03	2.54
2.00	1.50	3.00	0.03	3.39
2.00	1.00	4.00	0.04	4.24
2.00	1.00	5.00	0.05	5.08
2.50	1.50	6.00	0.06	5.93
3.00	2.00	7.00	0.07	6.78
3.50	1.50	8.00	0.08	7.63
3.50	2.50	9.00	0.08	8.47
3.50	2.00	10.00	0.09	9.32
4.00	3.00	11.00	0.10	10.17
4.00	2.00	12.00	0.11	11.02
4.00	2.50	13.00	0.12	11.86
4.00	3.50	14.00	0.13	12.71
4.50	3.50	15.00	0.14	13.56
4.50	3.00	16.00	0.14	14.41
5.00	3.00	17.00	0.15	15.25
5.00	4.50	18.00	0.16	16.10
5.00	5.00	19.00	0.17	16.95
6.00	5.00	20.00	0.18	17.80
7.00	2.50	21.00	0.19	18.64
7.00	4.50	22.00	0.19	19.49
7.00	5.00	23.00	0.20	20.34
7.00	3.00	24.00	0.21	21.19
8.00	7.00	25.00	0.22	22.03
8.00	2.00	26.00	0.23	22.88
9.00	5.00	27.00	0.24	23.73

9.00	4.00	28.00	0.25	24.58
9.00	9.00	29.00	0.25	25.42
9.50	4.00	30.00	0.26	26.27
10.00	10.00	31.00	0.27	27.12
10.00	6.00	32.00	0.28	27.97
10.00	7.00	33.00	0.29	28.81
10.00	7.00	34.00	0.30	29.66
10.00	7.00	35.00	0.31	30.51
12.00	7.00	36.00	0.31	31.36
12.00	5.00	37.00	0.32	32.20
12.00	5.00	38.00	0.33	33.05
14.00	9.00	39.00	0.34	33.90
14.00	7.00	40.00	0.35	34.75
14.50	9.00	41.00	0.36	35.59
15.00	14.00	42.00	0.36	36.44
15.00	10.00	43.00	0.37	37.29
16.00	9.00	44.00	0.38	38.14
17.00	10.00	45.00	0.39	38.98
17.00	14.50	46.00	0.40	39.83
18.00	13.00	47.00	0.41	40.68
20.00	15.00	48.00	0.42	41.53
22.00	10.00	49.00	0.42	42.37
22.00	13.00	50.00	0.43	43.22
24.00	23.00	51.00	0.44	44.07
30.00	15.00	52.00	0.45	44.92
31.00	12.00	53.00	0.46	45.76
33.00	20.00	54.00	0.47	46.61
33.00	18.00	55.00	0.47	47.46
33.00	27.00	56.00	0.48	48.31
33.00	27.00	57.00	0.49	49.15
36.00	16.00	58.00	0.50	50.00
40.00	20.00	59.00	0.51	50.85
40.00	20.00	60.00	0.52	51.69
44.00	40.00	61.00	0.53	52.54
45.00	33.00	62.00	0.53	53.39
46.00	30.00	63.00	0.54	54.24
50.00	30.00	64.00	0.55	55.08
50.00	29.00	65.00	0.56	55.93
62.00	46.00	66.00	0.57	56.78
64.00	45.00	67.00	0.58	57.63
66.00	45.00	68.00	0.58	58.47
77.00	57.00	69.00	0.59	59.32
95.00	26.00	70.00	0.60	60.17
97.00	58.00	71.00	0.61	61.02
100.00	72.00	72.00	0.62	61.86
100.00	60.00	73.00	0.63	62.71
100.00	62.00	74.00	0.64	63.56
100.00	62.00	75.00	0.64	64.41

113.00	86.00	76.00	0.65	65.25
115.00	65.00	77.00	0.66	66.10
119.00	79.00	78.00	0.67	66.95
122.00	94.00	79.00	0.68	67.80
123.00	93.00	80.00	0.69	68.64
127.00	60.00	81.00	0.69	69.49
127.00	60.00	82.00	0.70	70.34
128.00	104.00	83.00	0.71	71.19
128.00	87.00	84.00	0.72	72.03
134.00	45.00	85.00	0.73	72.88
135.00	95.00	86.00	0.74	73.73
135.00	93.00	87.00	0.75	74.58
143.00	80.00	88.00	0.75	75.42
143.00	80.00	89.00	0.76	76.27
150.00	40.00	90.00	0.77	77.12
160.00	140.00	91.00	0.78	77.97
160.00	144.00	92.00	0.79	78.81
185.00	142.00	93.00	0.80	79.66
213.00	159.00	94.00	0.81	80.51
221.00	168.00	95.00	0.81	81.36
223.00	201.00	96.00	0.82	82.20
224.00	223.00	97.00	0.83	83.05
224.00	178.00	98.00	0.84	83.90
224.00	176.00	99.00	0.85	84.75
228.00	147.00	100.00	0.86	85.59
231.00	103.00	101.00	0.86	86.44
234.00	132.00	102.00	0.87	87.29
234.00	184.00	103.00	0.88	88.14
236.00	132.00	104.00	0.89	88.98
240.00	186.00	105.00	0.90	89.83
248.00	176.00	106.00	0.91	90.68
309.00	274.00	107.00	0.92	91.53
320.00	245.00	108.00	0.92	92.37
328.00	264.00	109.00	0.93	93.22
332.00	233.00	110.00	0.94	94.07
335.00	278.00	111.00	0.95	94.92
340.00	260.00	112.00	0.96	95.76
398.00	253.00	113.00	0.97	96.61
422.00	100.00	114.00	0.97	97.46
452.00	420.00	115.00	0.98	98.31
456.00	340.00	116.00	0.99	99.15
478.00	355.00	117.00	1.00	100.00

Cross Section of Particles

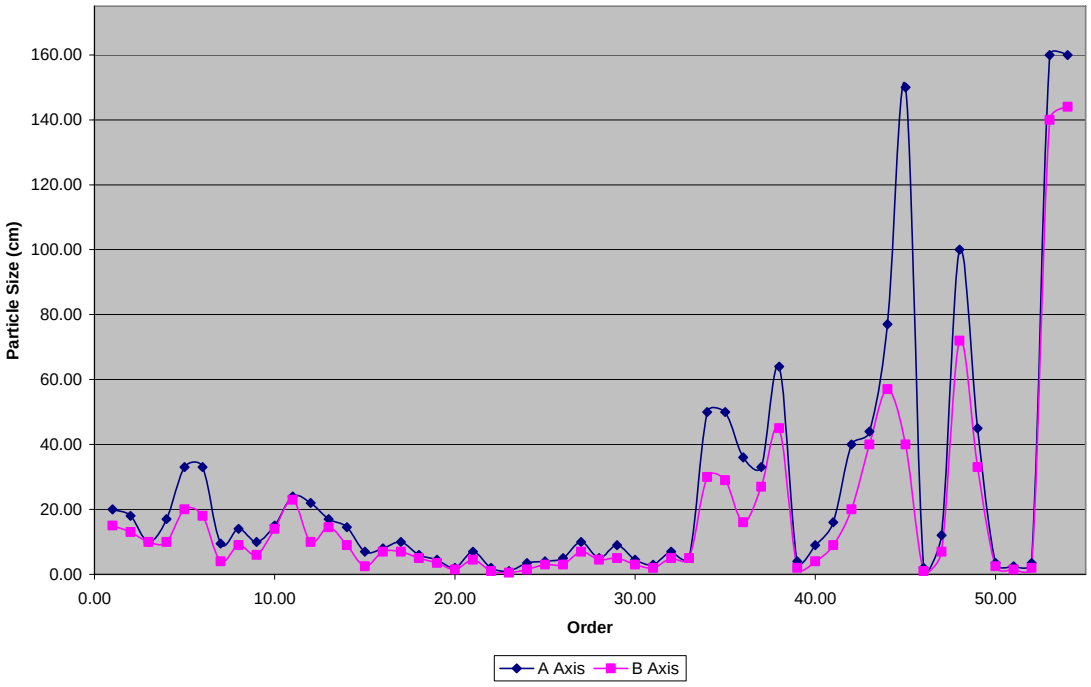

A vs. B Upper Reach

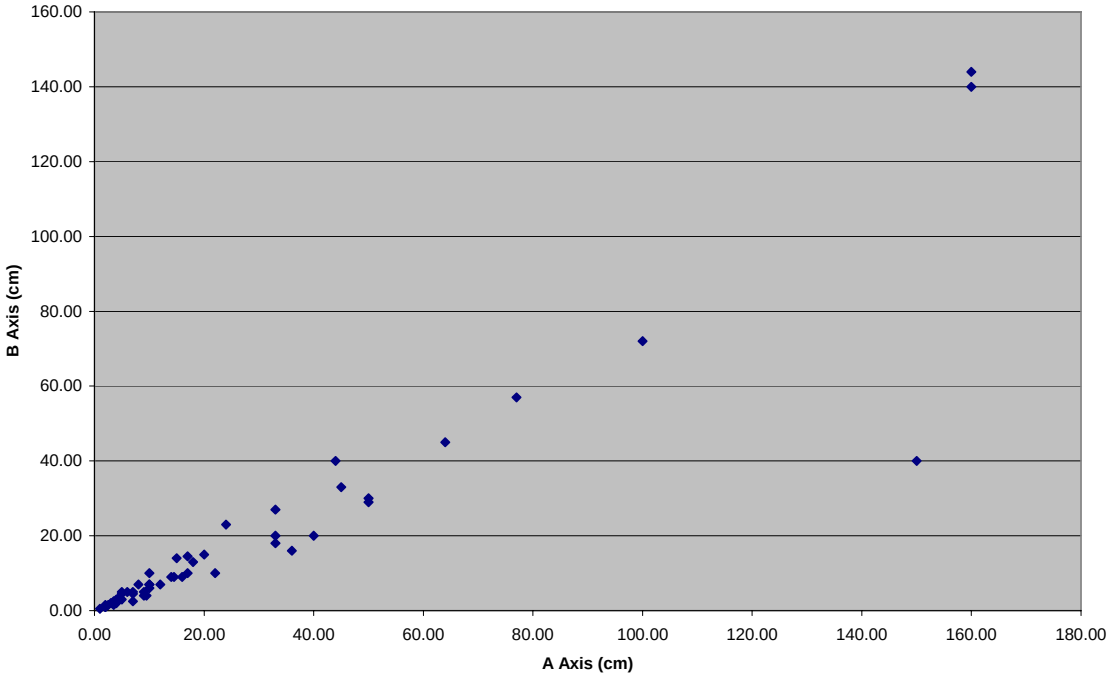

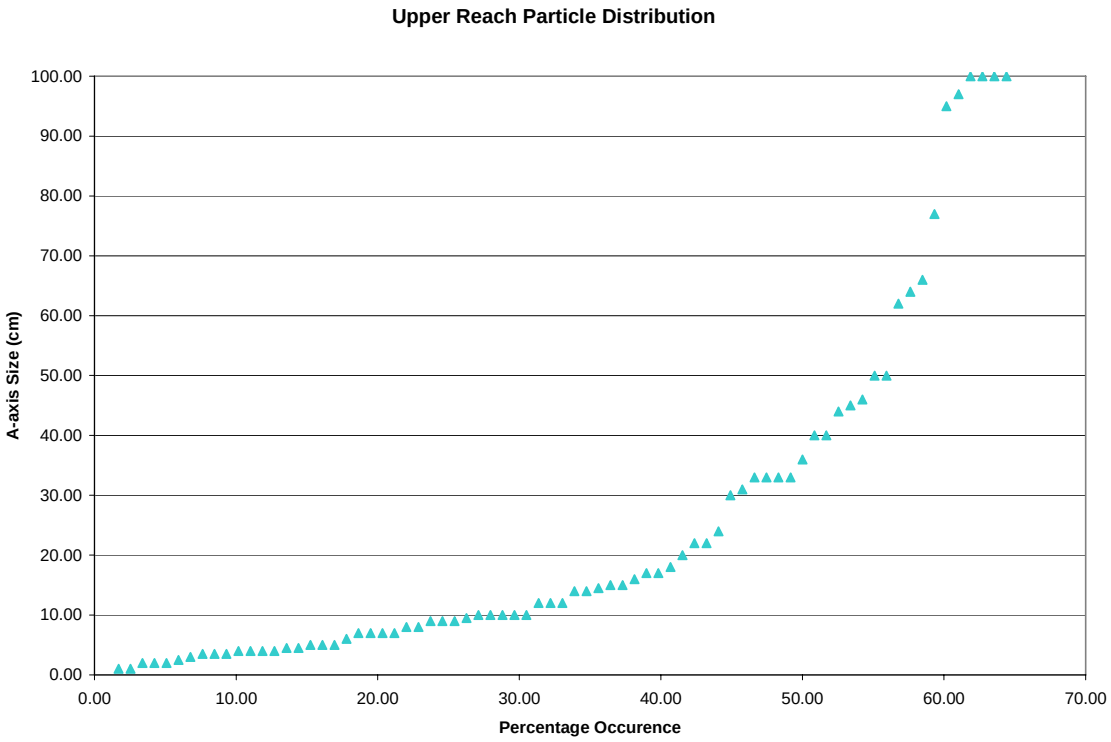

Lower Reach

Distance	Shear Stress per unit Width	T* D50	T* D84
(m)	N/m	.26 m	.56 m
0.00	0.00	0.0000	0.0000
0.30	299.21	0.0711	0.0330
0.61	363.33	0.0863	0.0401
0.91	299.21	0.0711	0.0330
1.22	341.96	0.0812	0.0377
1.52	414.62	0.0985	0.0457
1.83	470.19	0.1117	0.0519
2.13	418.90	0.0995	0.0462
2.44	453.09	0.1076	0.0500
2.74	470.19	0.1117	0.0519
3.05	440.27	0.1046	0.0486
3.35	376.15	0.0893	0.0415
3.66	512.94	0.1218	0.0566
3.96	517.21	0.1228	0.0570
4.27	508.66	0.1208	0.0561
4.57	495.84	0.1178	0.0547
4.88	500.11	0.1188	0.0552

5.18	427.45	0.1015	0.0471
5.49	380.43	0.0904	0.0420
5.79	423.17	0.1005	0.0467
6.10	512.94	0.1218	0.0566
6.40	461.64	0.1096	0.0509
6.71	542.86	0.1289	0.0599
7.01	517.21	0.1228	0.0570
7.32	577.05	0.1371	0.0636
7.62	551.41	0.1310	0.0608
7.93	688.19	0.1635	0.0759
8.23	649.72	0.1543	0.0716
8.54	645.44	0.1533	0.0712
8.84	632.62	0.1503	0.0698
9.15	641.17	0.1523	0.0707
9.45	653.99	0.1553	0.0721
9.76	649.72	0.1543	0.0716
10.06	641.17	0.1523	0.0707
10.37	598.43	0.1421	0.0660
10.67	611.25	0.1452	0.0674
10.98	641.17	0.1523	0.0707
11.28	624.07	0.1482	0.0688
11.59	577.05	0.1371	0.0636
11.89	606.97	0.1442	0.0669
12.20	624.07	0.1482	0.0688
12.50	619.80	0.1472	0.0683
12.80	606.97	0.1442	0.0669
13.11	611.25	0.1452	0.0674
13.41	615.52	0.1462	0.0679
13.72	598.43	0.1421	0.0660
14.02	624.07	0.1482	0.0688
14.33	611.25	0.1452	0.0674
14.63	577.05	0.1371	0.0636
14.94	611.25	0.1452	0.0674
15.24	465.92	0.1107	0.0514
15.55	418.90	0.0995	0.0462
15.85	423.17	0.1005	0.0467
16.16	457.37	0.1086	0.0504
16.46	179.53	0.0426	0.0198
16.77	149.61	0.0355	0.0165
17.07	64.12	0.0152	0.0071
17.38	29.92	0.0071	0.0033
17.68	8.55	0.0020	0.0009
17.99	4.27	0.0010	0.0005
18.29	85.49	0.0203	0.0094
18.60	192.35	0.0457	0.0212
18.90	205.17	0.0487	0.0226
19.21	166.70	0.0396	0.0184
19.51	218.00	0.0518	0.0240

19.82	141.06	0.0335	0.0156
20.12	123.96	0.0294	0.0137
20.43	132.51	0.0315	0.0146
20.73	106.86	0.0254	0.0118
21.04	102.59	0.0244	0.0113
21.34	81.21	0.0193	0.0090
21.65	59.84	0.0142	0.0066
21.95	29.92	0.0071	0.0033
22.26	4.27	0.0010	0.0005
22.56	0.00	0.0000	0.0000

A-Axis	B-Axis	A	B	Order
		//	*//*	
3.15	1.4	*		1
0.62	0.35	*		2
0.55	0.49	*		3
0.5	0.36		*	4
0.25	0.19	*		5
0.24	0.1	*		6
1.1	0.46		*	7
0.13	0.12		*	8
0.07	0.07		*	9
0.29	0.18	*		10
0.23	0.19	*		11
0.18	0.19	*		12
0.1	0.19	*	*	13
0.26	0.17		*	14
0.11	0.08		*	15
0.56	0.26			16
0.2	0.13	*		17
2.16	0.74		*	18
0.5	0.43	*		19
0.22	0.16		*	20
0.34	0.47			21
0.53	0.26		*	22
0.51	0.29		*	23
1.17	0.6	*		24
0.17	0.6	*		25
0.16	0.09		*	26
0.28	0.2		*	27
0.36	0.21		*	28
0.26	0.18		*	29
0.24	0.17		*	30
1.43	0.86	*		31
0.4	0.28			32
0.32	0.22		*	33
0.37	0.31		*	34

0.28	0.1		*	35
0.12	0.08		*	36
0.17	0.12		*	37
0.28	0.26	*		38
0.21	0.19	*		39
0.13	0.14	*		40
4.78	1.42	*		41
2.48	1.35	*		42
0.28	0.17	*		43
0.23	0.17	*		44
0.35	0.21		*	45
0.33	0.14		*	46
0.28	0.23		*	47
0.12	0.08	*		48
0.17	0.13	*		49
1.73	0.75	*		50
0.29	0.14	*		51
0.04	0.035	*		52
0.07	0.06	*		53
0.045	0.02	*		54
0.08	0.075	*		55
0.03	0.02	*		56
0.08	0.06	*		57
0.13	0.07	*		58

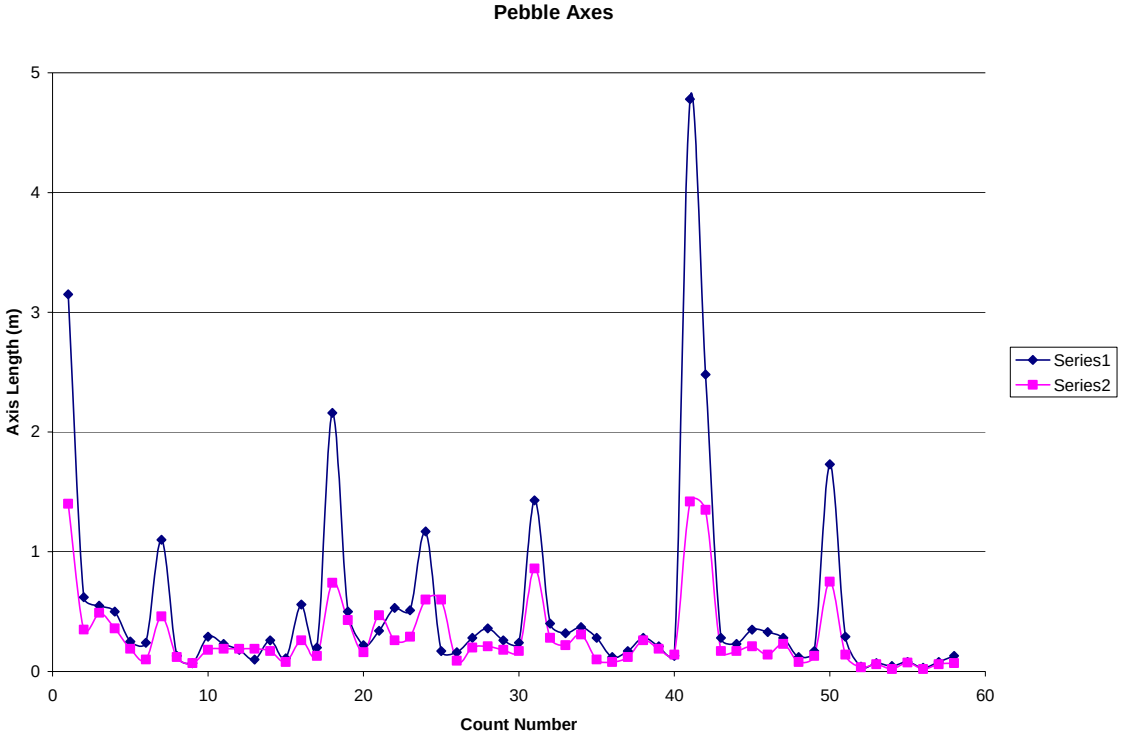

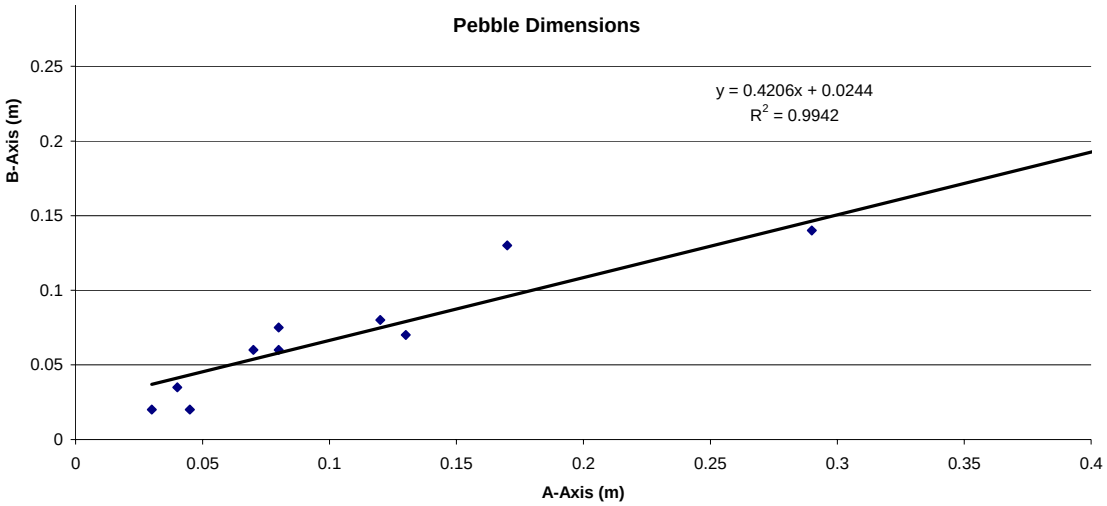
Pebble Dimensions
y = 0.4206x + 0.0244
R2 = 0.9942
B-Axis (m)
A-Axis (m)
0
0.05
0.1
0.15
0.2
0.25
0.3
0.35
0.4

Appendix 5: Depth and Widths

Widths

Distance Downstream	Effective width	Channel width	Bed Material	Stream Power	Stream Power
(m)	(m)	(m)		per width	per width effective
16.95	14.33	14.33	bedrock	11.02	11.02
17.50	10.97	18.29	bedrock	8.63	14.38
26.70	12.80	31.55	boulders/sand	5.00	12.33
38.28	24.38	33.22	boulders/cobbles	4.75	6.47
44.38	6.40	31.39	boulders	5.03	24.65
51.21	17.37	36.58	boulders	4.31	9.08
57.21	12.37	38.25	boulders	4.13	12.75
51.61	18.59	32.31	boulders	4.88	8.49
54.96	16.76	29.72	boulders	5.31	9.41
65.23	9.60	22.25	boulders	7.09	16.44
64.00	5.02	22.56	boulders	6.99	31.42
75.29	5.09	20.12	bedrock	7.84	31.00
75.00	7.62	19.51	bedrock	8.09	20.71
83.21	7.92	16.31	bedrock	9.68	19.91
82.80	24.20	29.00	boulders	5.44	6.52
92.35	25.30	25.30	boulders	6.24	6.24
85.88	33.65	33.65	boulders	4.69	4.69
98.45	26.80	26.82	bedrock/boulder	5.88	5.89
106.07	25.90	25.30	boulders/cb	6.24	6.09
113.69	35.60	35.66	cobbles/bld	4.42	4.43

Longitudinal Profile of Effective and Actual Widths

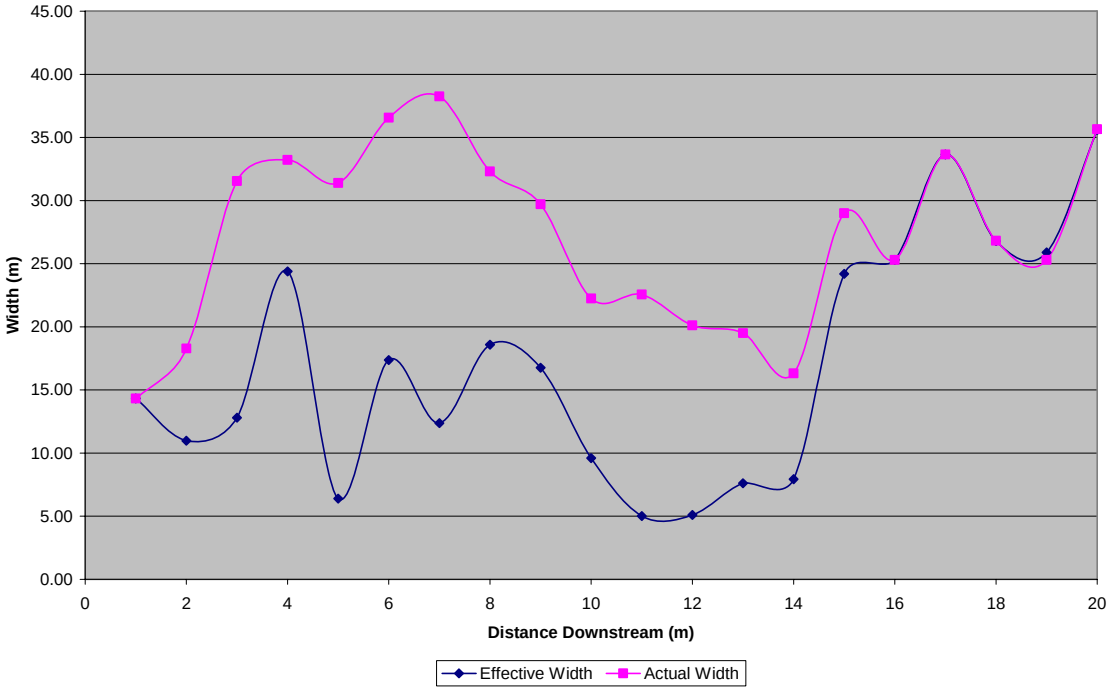

Longintudinal Profile of Stream Power per unit Width

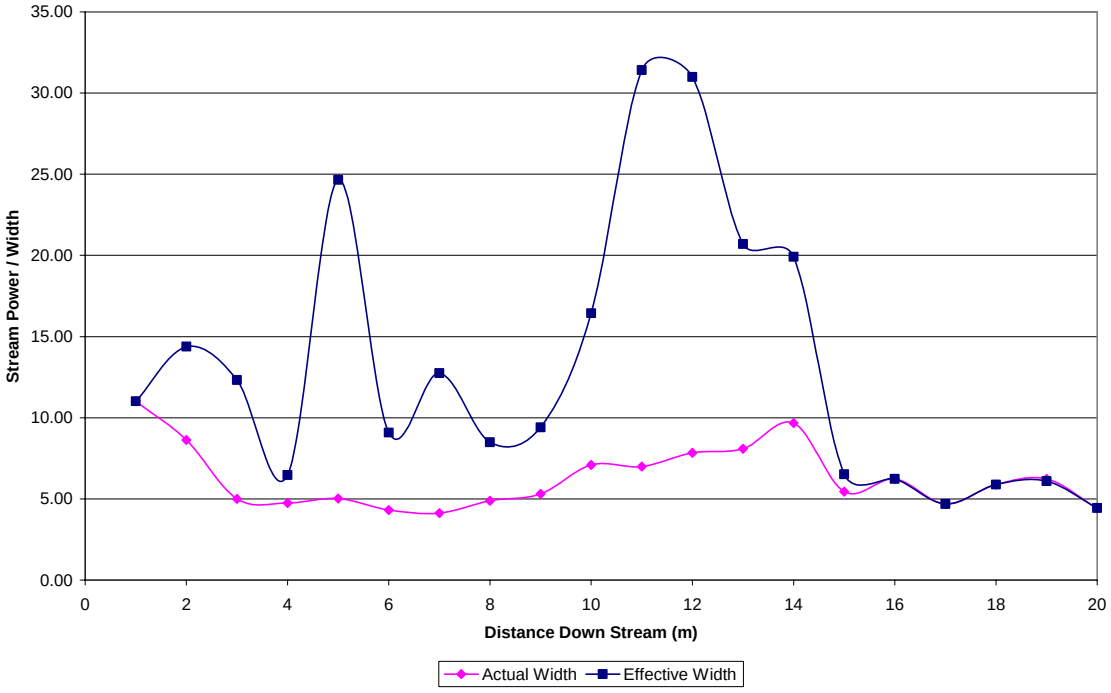

Depths

Distance (m)	Upper/ Middle Lower	Width (m)	Depth (m)	Area (m^2)	Discharge (cubic m/s)	Velocity (m/s)	Froude Number
17.50	U	18.28	1.30	23.76	157.80	6.64	2.25
64.00	U	22.56	1.50	33.84	157.80	4.66	1.11
70.00	M	10.00	2.00	20.00	157.80	7.89	3.17
75.00	L	19.51	3.70	72.19	157.80	2.19	0.24
82.80	L	29.00	2.50	72.50	157.80	2.18	0.24
85.88	L	33.65	2.90	97.59	157.80	1.62	0.13

Appendix 6: Pictures

Flood Pictures: Up Stream to Down Stream

Overland flow

Flow out of Largest Knickpoint

Variance in flood width

Upper reach flood

Standing Waves

Plunging flow over Boulder Knickpoint

Down Stream Skimming Flow

Low Flow Pictures
Upstream to Downstream

Flood on April 22nd, looking down stream

Low flow looking upstream

Recirculation Eddy Deposit

Looking downstream to particle jam

Particle Jam

Top of Particle Jam looking Down Stream

Width of Boulder Knickpoint

Particle Jam Flood Picture 4/22

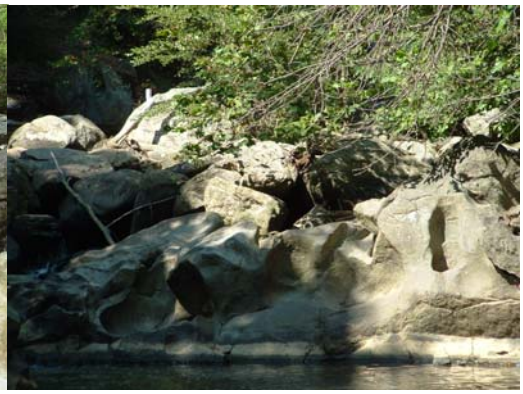

Bedrock and Particle Knickpoint

April 22 flood over knickpoint and lower reach

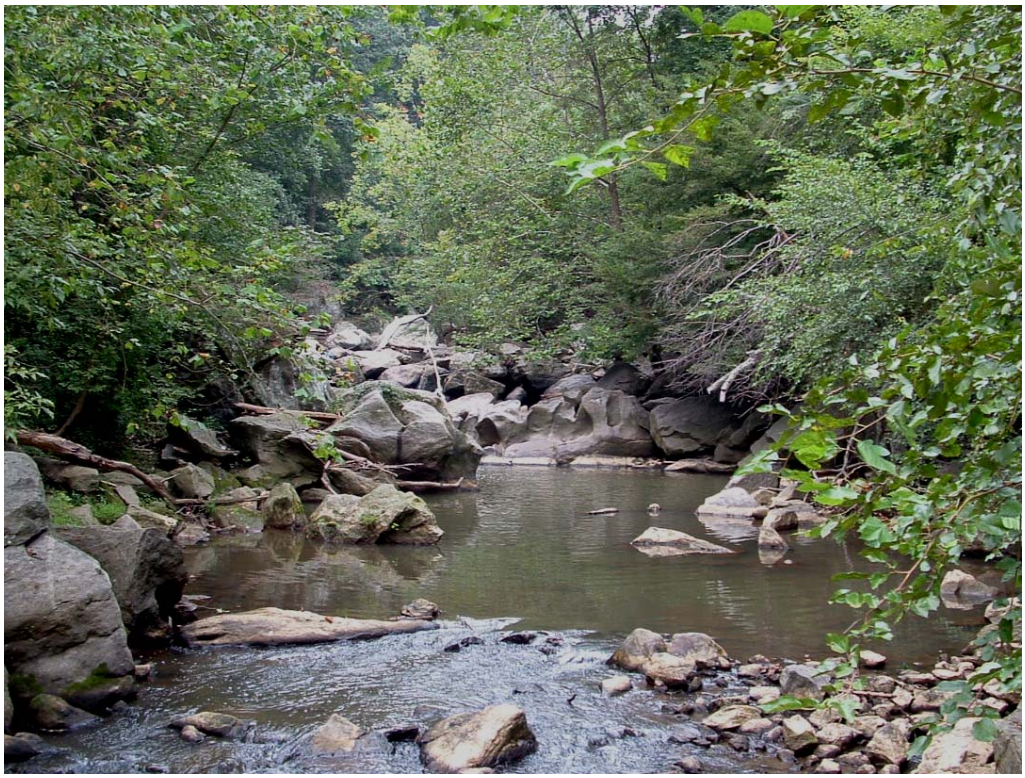

End of surveyed area looking upstream

Paleoarc

Overturned Pothole Sediment in bedload trapped in Pothole

Appendix 7: Honor Code

I pledge on my honor that I have not given nor received any unauthorized assistance on this assignment.